LaNi 5 related AB 5 compounds: structure, properties and applications

Jean-Marc Joubert, Valérie Paul-boncour, Fermin Cuevas, Junxian Zhang, Michel Latroche

$LaNi_5$ related AB_5 compounds: structure, properties and applications

Paper dedicated to Annick Percheron-Guégan in the occasion of her 80th birthday

Jean-Marc Joubert*, Valérie Paul-Boncour, Fermín Cuevas, Junxian Zhang, Michel Latroche

Univ Paris Est Creteil, CNRS, ICMPE, UMR 7182, 2 rue Henri Dunant, 94320 Thiais, France

*corresponding author: joubert@icmpe.cnrs.fr

Abstract
This paper is a comprehensive review of the properties of $LaNi_5$ derivatives and other AB_5 compounds with $CaCu_5$ crystal structure (*A*=Y, lanthanide, Th and *B*=transition metal, Al, Ge, Si, Sn) and their applications. The crystal structures of the intermetallic compounds are described considering their chemical composition and off-stoichiometry. Same approach is conducted for the metallic hydrides formed by direct reaction of dihydrogen with the intermetallic. The thermodynamic properties of the sorption reaction are presented regarding equilibrium pressure and reversibility. In a second step, outstanding applications are given focusing first on magnetic properties and electrochemical energy storage. Finally, other uses such as gas storage, heat exchange, compression or gas separation and purification are highlighted showing the tremendous possibilities offered by this class of materials.

1. Introduction

AB_5 compounds with $CaCu_5$ crystal structure and their derivatives have a very rich chemistry and outstanding properties. $LaNi_5$ is known in particular as a prototype of hydrogen absorbing and hydride forming intermetallic compounds. Its derivatives were also among the first to be used for the electrochemical application of nickel-metal hydride (Ni-*M*H) batteries. The magnetic properties in the $CaCu_5$ family are also extremely rich.

The present paper is a review highlighting the structural properties of intermetallic compounds and hydrides, the thermodynamic properties of hydrogen absorption and the magnetic properties of AB_5 compounds as well as electrochemical and other applications. This will be done with a particular focus on $LaNi_5$ compound and its substitutional derivatives. The work done in the *Laboratoire de Chimie Métallurgique des Terres Rares* under the supervision of Annick Percheron-Guégan will be particularly highlighted.

For a more detailed review, the reader is referred to [1]. The structural properties of the intermetallic compounds and the hydrides will be first reviewed. Then, the thermodynamic properties and magnetic properties will be presented. Finally, we will focus on applications with a special emphasis on the electrochemical application for Ni-*M*H batteries.

2. Structural Properties

2.1 Intermetallic compounds

The $CaCu_5$ family is very rich. 117 binary compounds have been reported with this hexagonal crystal structure described in *P*6/*mmm* (191) space group [2]. The crystal structure represented in Fig. 1 is very simple. The large atom (generally a rare earth, *RE*) occupies site 1*a* and the smaller atom (generally a transition metal) sites 2*c* and 3*g*.

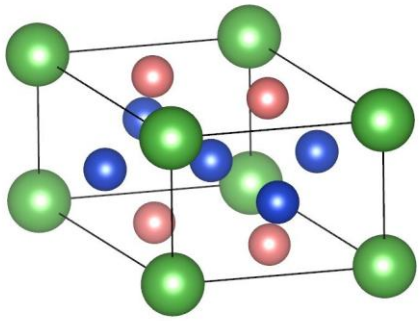

Fig. 1. Crystal structure of $LaNi_5$: La in 1*a* (green), Ni in 2*c* (salmon) and 3*g* (blue).

As we will see, chemical substitution is the most efficient way to tune the properties for applications. Therefore, the structure of substituted compounds is interesting to study.

If we consider the case of the prototypic compound $LaNi_5$, from the ternary phase diagrams point of view, the situation is as follows. Lanthanum can be completely replaced by substitution by all the other *RE* elements. The substitution of the nickel is however most often limited. Cobalt [3], copper [4], zinc [5] and platinum [6] are examples of transition elements able to replace nickel completely. On the other hand, manganese [7], iron [8] and aluminum [9] substitutions are limited (see Table 1). This makes the study of the ternary phase diagrams based on La–Ni system particularly rich and interesting [10].

Table 1
Solubility limit *x* and site preference for chemical substitution in $LaNi_{5-x}M_x$ ternary compounds.

Substituting element *M*	Substitution limit *x*	Site preference 2*c* or 3*g*	Reference
Al	1.25	complete order on 3*g*	[9]
Au	1.5	complete order on 3*g*	[10]
Co	5	slight preference for 3*g*	[3,11]
Cu	5	equal occupancy of 2*c* and 3*g*	[4,12]
Fe	1.2	strong preference for 3*g*	[8]
Ge	0.5	complete order on 3*g*	[13]
Ir	2.5 and from 4 to 5	complete order on 3*g*	[10]
Mn	2	strong preference for 3*g*	[7]
Pd	1.6	slight preference for 3*g*	[10]
Pt	5	complete order on 3*g*	[6]
Rh	3	strong preference for 3*g*	[10]
Ru	0.5	complete order on 3*g*	[10]
Si	0.5	complete order on 3*g*	[12]
Sn	0.5	complete order on 3*g*	[14]
Zn	5	unknown	[5]

From the crystallographic point of view also, the situation is complex. The question of the position of the substituting element is important because it can also be related to the properties (hydrogen storage properties and structural properties of the hydrides). Since there are two available sites 2*c* and 3*g*, the substitution can, in principle, occur either in one of the two sites or in both sites simultaneously. This can be studied by X-ray diffraction when the diffraction contrast between elements is sufficient. Otherwise, neutron diffraction may be used (in particular for other 3*d* metals). Detailed crystallographic study shows that the substitution on site 2*c* only is never observed. The substitution can occur on site 3*g* only (in the case of Pt [6] and Ir for example). But the most frequent case is that it occurs on both

sites with a preference for site 3*g*. In few cases, no preference is observed, and the distribution is almost statistical (Co, Cu). A summary of the findings from the literature is presented in Table 1.

Few studies are devoted to multinary systems in which more than one substituting element is present. An exception is the study of the famous $LaNi_{3.55}Mn_{0.4}Al_{0.3}Co_{0.75}$ [15] whose electrochemical properties are remarkable and which is the base of the compounds actually used in Ni-*M*H batteries (see Section 5). For this complex case, X-ray or neutron diffraction only is not sufficient to achieve the distribution of the elements. Resonant diffraction was therefore used with different measurements done at the K-edges of the different 3*d* elements. This successfully led to the complete picture of the atomic distribution which is actually found to be closely related to that observed for mono-substituted compounds.

Another important consequence of the substitution is the modification of the cell volume as a function of composition. Linear trends are generally found with different slopes in accord with the size of the substituting element *i.e.* roughly, the cell volume is proportional to the content and the atomic size of the substituting element (Vegard's law) [1]. Fig. 2 shows the cell volume of $LaNi_{5-x}M_x$ as a function of the substitution rate.

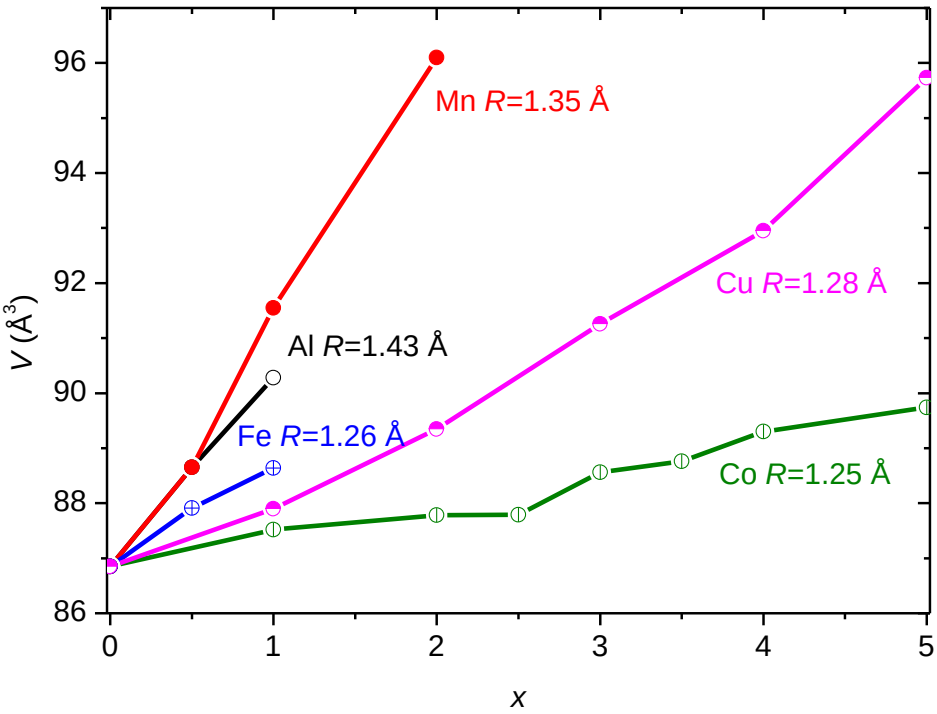

Fig. 2. Cell volume as a function of substitution rate of $LaNi_{5-x}M_x$ ternary compounds with indication of the atomic radii (R_{Ni}=1.24 Å) [3,4,7,9,16,17].

But, the individual lattice parameters may have a strongly different behavior from the linear one. In this regard, the example of platinum substitution is particularly striking. The system La–Ni–Pt is remarkable since $LaPt_5$ has the same crystal structure as $LaNi_5$ leading to a complete substitution range between the two binary compounds. The lattice parameters are shown in Fig. 3 and it is clearly seen that their variations have to do with the site occupancies reported in the same figure [6]. Due to geometric considerations, the *a* lattice parameter is more sensitive to the occupancy on site 3*g* while the *c* parameter is more sensitive to the occupancy on site 2*c*. The non-homogeneous substitution with an order of Pt in site 3*g* causes a non-regular variation of *a* and *c* parameters particularly well shown on the plot of *c*/*a*. However, overall, the cell volume follows a regular (and very strong) increase related to the difference of atomic radii between Ni (1.24 Å) and Pt (1.30 Å).

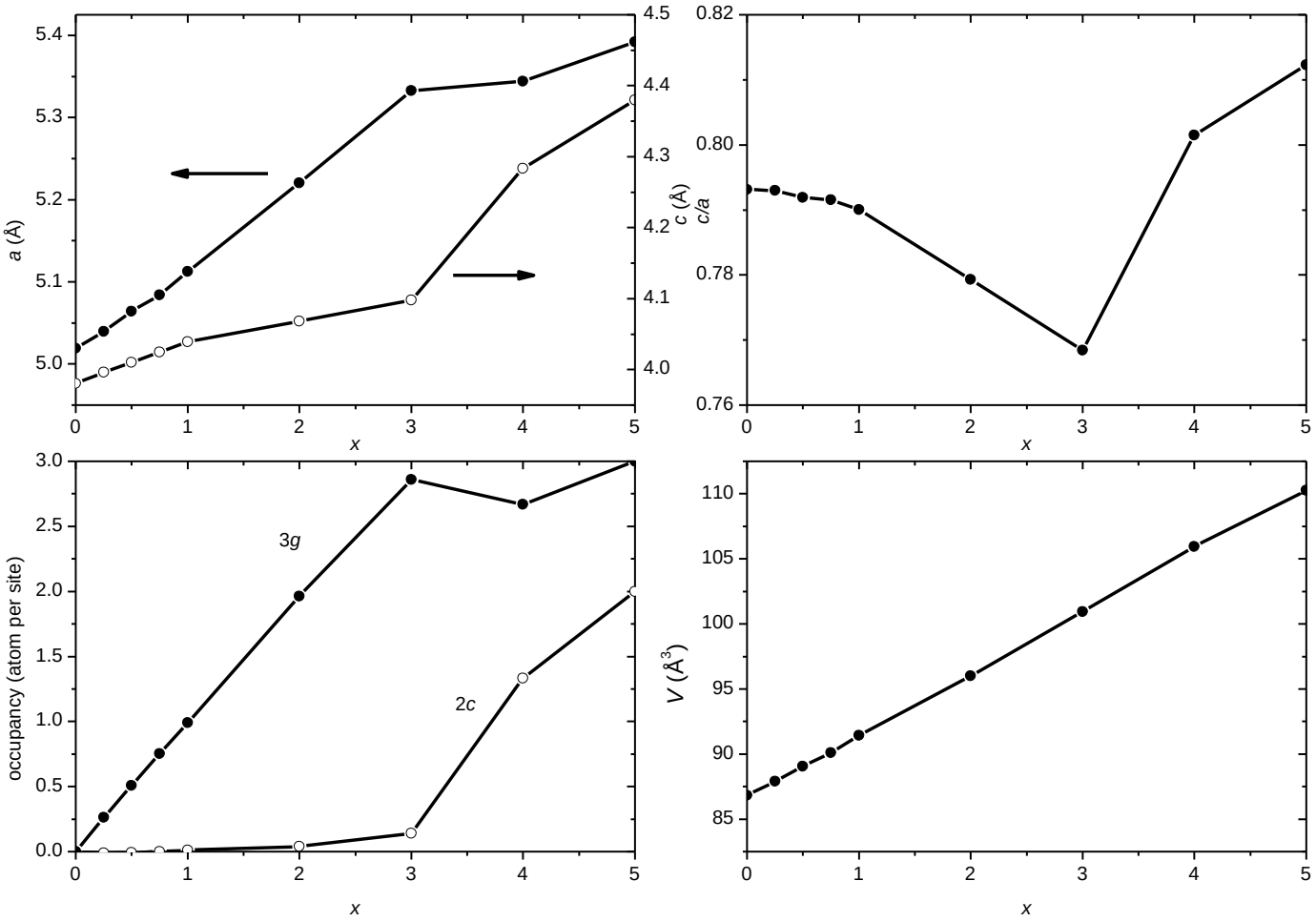

Fig. 3. Lattice parameters, *c*/*a*, site occupancies and cell volume of $LaNi_{5-x}Pt_x$ compounds.

A peculiarity of AB_5 compounds with the $CaCu_5$ structure is the possibility to accommodate a significant range of non-stoichiometry reflected by changes of the *B*/*A* ratio. Contrary to most intermetallic compounds that accommodate non stoichiometry by simple mechanisms such as interstitials, vacancies or anti-site defects (substitution), $CaCu_5$ structure adopts a more complex scheme. *RE* atoms are replaced not by a single transition metal atom but by a pair of atoms (called dumbbell) oriented along the *c* axis. Contrary to a simple substitution mechanism, two atoms replace one and obviously the two atoms cannot occupy the *RE* positions implying the occupancy of a new site in the crystal structure (2*e*) and a vacant position at the *RE* site (1*a*). The presence of this vacant site has a consequence also on the transition metal position since it is found that the surrounding hexagon around 1*a* position shrinks. This provokes the occupation of a new site 6*l* and site 2*c* is therefore not fully occupied. The composition can be expressed as $\mathrm{La}_{1-s}^{1a}\mathrm{Ni}_{2s}^{2e}\mathrm{Ni}_{2-6s}^{2c}\mathrm{Ni}_{6s}^{6l}\mathrm{Ni}_{3}^{3g}$.

A drawing of the structure is given in Fig. 4. The mechanism has been first proposed by Buschow [18] and is fully described and refined in the case of $LaNi_{5+x}$ compounds in Ref. [19]. The local correlation between missing atom in 1*a* position and shrunk 6*l* hexagon has been proved in Ref. [20] in the case of Yb–Cu system using the Pair Distribution Function. This model is valid only for a limited fraction of dumbbells. For higher content, there is a tendency to ordering. This yields a few possible structures ($LuFe_{9.5}$, $PrFe_7$, Th_2Ni_{17}, Th_2Zn_{17}...) some of which have interesting hydrogen storage or magnetic properties out of the scope of the present article. In the case of $LaNi_5$, the non-stoichiometry is limited to $LaNi_{5.4}$ for stable alloys. In contrast, using non-equilibrium synthetic routes, non-stoichiometry up to $LaNi_{9.2}$ has been reported for this compound [21,22].

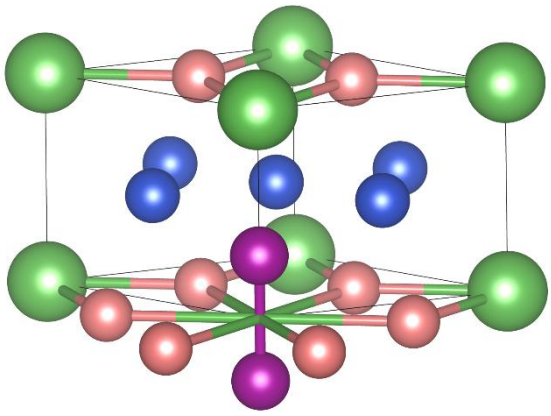

Fig. 4. Crystal structure model of the non-stoichiometric $LaNi_5$ phase: La in 1*a* (green), Ni in 2*c* and 6*l* (salmon), 3*g* (blue) and 2*e* (purple).

2.2 Hydrides

The basic model for the understanding of the structure of the hydrides of AB_5 compounds is that of $LaNi_{4.5}Mn_{0.5}D_{6.6}$ [7]. It is a four-site interstitial model keeping the space group of the original compound. Hydrogen (deuterium) atoms are distributed into these sites with different site occupancies always very far from full occupancy (the maximum site occupancy is ~40%). The reasons explaining the non-complete occupancies are found in the well-known criteria for occupation of a position in metal hydrides: hydrogen atoms should not be closer than 2.1 Å and the site size should be larger than 0.4 Å [23,24]. This results in a kind of disordered, liquid-like lattice inside the well-ordered framework represented by the metallic atoms. The structure is drawn in Fig. 5.

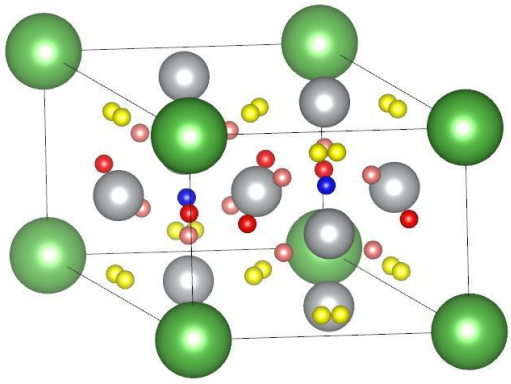

Fig. 5. Structure of $LaNi_5D_5$: D in 4*h* (blue), 6*m* (red),12*n* (yellow) and 12*o* (salmon).

The four sites have different coordinations: A_2B_2 for 6*m*, AB_3 for 12*n* and 12*o* and B_4 for 4*h*. The site coordinated by A_2B_2 has always the largest hydrogen occupancy, as expected from the higher chemical affinity related to the higher number of *RE* elements in the coordination sphere correlated with a larger size of the interstitial site. The determination of site occupancies as a function of the substituting element in $LaNi_5$ and the rate of substitution has been the subject of numerous studies [7,12–14,25–30]. It is shown in particular that elements with a repulsive character towards hydrogen may deplete the interstitial sites they coordinate. We can see here that there is also an evident relation to the substitution site of this metallic element as studied in Section 2.1 making this determination very important.

Different structure models are found when deuterium atoms order. The most simple ordering is found in the case of $LaNi_5D_5$ [31]. The symmetry decrease is promoted by the elimination of the mirror perpendicular to the *c* direction. This ordering is also observed in the case of $LaNi_{4.9}Al_{0.1}$ [28], $LaNi_{4.75}Pd_{0.25}$ [30], $LaNi_{4.75}Pt_{0.25}$ [6], $LaNi_{4.8}Sn_{0.2}$ [14,32].

More complex structure is observed in the case of the higher hydride of $LaNi_5$ with 6.7 D per formula unit (f.u.). In the model proposed in Refs. [31,33,34] and further refined in Ref. [35], 7 sites are occupied. Both a symmetry reduction and cell doubling are observed related to ordering. Note that ordering is still partial and that completely ordered structures (with complete occupancy of several deuterium sites) are never observed.

Other complex models may be found in special cases like $LaCu_5D_{3.2}$ [36], $LaNi_{4.25}Pt_{0.75}D_{2.61}$ [6] or $LaNi_4PdD_{2.72}$ [30].

One of the parameters having a high importance on the properties (in particular the electrochemical properties) is the change of the volume after hydriding. In some cases, it is not only the global volume change between the metal lattice and the fully hydrogenated hydride, but rather the discrete volume change occurring in the plateau region corresponding to phase transformation that is important for cycle-life properties. It can be as high as 22.4% and as low as 9.9%. The role of cobalt in this reduction of the discrete lattice expansion has been particularly emphasized [37].

3. Thermodynamic properties

$LaNi_5$ binary compound itself has outstanding hydrogen absorption properties. It has first a large absorption capacity of ~6.7 H/f.u. *i.e.* over 1 H/M, the largest observed in the $CaCu_5$ family. Moreover, the absorption plateau pressure is very close to ambient pressure at room temperature. This makes in principle this compound a good choice for applications in ambient conditions and the prototype of metal hydride forming intermetallic compounds.

The absorption thermodynamic properties are also remarkable. $LaNi_5$-hydrogen system shows a single flat plateau at room temperature extending from the saturated alpha phase (~0.3 H/f.u.) to the hydrogen rich beta phase (~6 H/f.u.). The fact that hydrogen can be stored and released within a very small pressure range is obviously very good also for applications in spite of the hysteresis. $LaNi_5$ hydrogen absorption curve with its simplicity and regularity resembles that of pure palladium, another prototype of hydrogen absorbing material. The pressure-composition curve is given in Fig. 6.

At higher temperature (80°C) a new hydride with the composition $LaNi_5H_3$ is formed [38]. This so-called γ hydride is important because it may have a relation with the intermediate phase sometimes formed in the electrochemical charging of AB_5 hydrides (see Section 5).

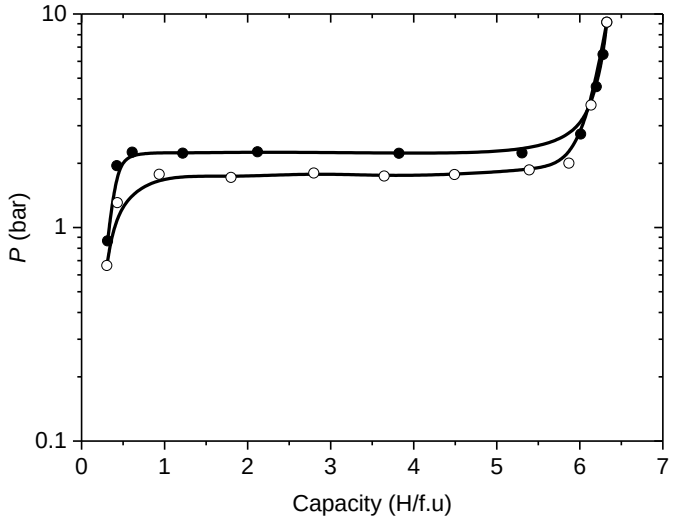

Fig. 6. Pressure-composition absorption-desorption curve for $LaNi_5$ at 25°C [39].

Even more remarkable is the fact that substitutions in $LaNi_5$ can substantially change the hydrogenation properties allowing to tune them to a large extent. As we have seen, many elements can substitute either La or Ni giving rise to the possibility of large changes of the properties. Unfortunately, the hydrogen storage capacity can never be increased by substitution. It is reduced more or less depending on the element (*e.g.* Al reduces a lot while Mn allows to keep a constant capacity). But the most striking effect of substitution on the hydrogen storage properties is shown on the changes of the plateau pressure which can reach several orders of magnitude. The example shown in Fig. 7 testifies for the effect of aluminum substitution. One may see the strong effect on both the plateau pressure and the capacity. Substitution on the rare earth site is also possible and may also control the equilibrium pressure [40].

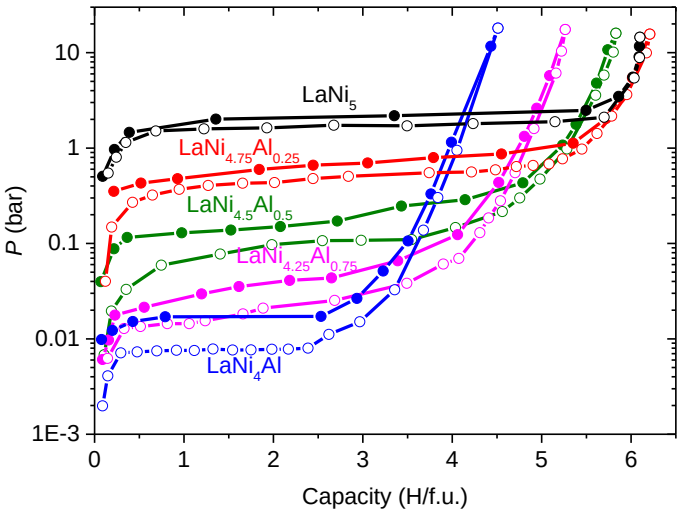

Fig. 7. Pressure-composition absorption-desorption curves of $LaNi_{5-x}Al_x$ compounds [9,41].

It is sometimes difficult to rationalize the changes of the capacity due to substitution, which are related to the change of the electronic properties. For the plateau pressure, related, through the Van't Hoff law, to the enthalpy of formation of the hydride, more regular rules are found. For example, it was observed that the logarithm of the plateau pressure generally varies linearly with the substitution rate of a given element. As the volume of the intermetallic compound varies also linearly with the composition (Vegard's law [42]), there is therefore a linear trend between the logarithm of the plateau pressure and the cell volume of the compound. The most remarkable finding was that the coefficient of proportionality is the same for many different elements giving rise to the so-called 'geometrical model' that allows to predict the plateau pressure as a function of the only measurement of the cell volume of the intermetallic compound which is easily accessible from diffraction [43–46]. This is a very practical and useful way to anticipate the properties. Unfortunately, it was later found that the model is not universal and that the slope of the linear dependence can change with the nature of the substitution element [6,26,30,47,48].

Finally, the use of very high pressures is a way to substantially increase the hydrogen storage capacity. It has been calculated, from geometrical considerations, that the limiting capacity is 9 H/f.u. [49]. This limit has indeed been reached or approached in a couple of experimental studies up to 1500 bar ($LaNi_5H_8$, $LaCo_5H_9$) [49] or 2500 bar ($CeNi_5H_{7.1}$, $LaCo_{4.95}Mn_{0.05}H_8$) [50], usually thanks to the existence of additional pressure plateaus. As far as we are aware, no structural study by neutron diffraction has been undertaken at these pressures in order to verify the structural model proposed by Lakner *et al.* [49]. In spite of these very high capacities, maintaining so high pressures is difficult and limits the practical application of these super-hydrides.

4. Magnetic properties of AB_5 compounds and their hydrides

The physical properties of AB_5 compounds with $CaCu_5$ crystal structure have been mainly studied for *A* = Th, *RE* and *B* = Co and Ni, which are particularly interesting as concern permanent magnets ($SmCo_5$) and hydrogen storage ($LaNi_5$) applications. The only known AFe_5 compound is $ThFe_5$, and few studies have been performed on this compound and its corresponding hydrides. We will briefly summarize its magnetic properties and give then a more detailed report on the electronic and magnetic properties of ACo_5 and ANi_5 type compounds and their hydrides. Extensive reviews of the physical properties of AB_5 intermetallic compounds and their hydrides can be found in Refs. [51–55]

4.1. AFe_5 compounds

$ThFe_5$ has a complex ferrimagnetic structure with T_C = 680 K. Its easy axis of magnetization determined by means of the Mössbauer spectroscopy and X-ray diffraction is found in the basal plane [56]. Hydrogen absorption leads to a rise in cell volume of 6%, a slight increase of the magnetization and Curie temperature with an easy axis aligned along the *a* axis [57].

4.2 ACo_5 compounds

The discovery in the 1970's of a very large uniaxial anisotropy, generating large coercive fields at room temperature, in ACo_5 intermetallics was a breakthrough in the field of permanent magnets. The BH_{max} factor, which was below 10 MGOe (80 kJ/m^3) for AlCoNi magnets, was progressively increased to 33 MGOe in optimized $SmCo_5$ type magnets and other *RE*-Co magnets ($RECo_5$, RE_2Co_{17}) [58]. Then, after 1985, the $SmCo_5$ type magnets were progressively replaced by sintered $NdFe_{14}B$ type magnets which can reach 50 MGOe and are constituted of less expensive elements [59]. A review on the *RE*-Co permanent magnets, their discovery, development, synthesis and applications can be found in Ref. [60]. $SmCo_5$ crystallizes in the $CaCu_5$ structure and is a ferromagnet with T_C around 1000 K, a saturation magnetization of 7.7 μ_B and a large uniaxial anisotropy with an easy *c*-axis (K_1= 11-20 10^7 erg cm^{-3}, H_A = 250-440 kOe) [60]. The outstanding magnetic properties of the ACo_5 compounds with light *RE* elements (*A* = Y, Ce, Pr, Nd, Sm) (High T_C, large M_S and coercive fields) [61–63] are lost for heavy *RE*, due to the 4f-3d ferrimagnetic coupling which generates a decrease of

the total magnetization at room temperature. The large uniaxial anisotropy in these hexagonal phases arises from both the light rare earths (*LRE*) dominant at low temperature and cobalt dominant at room temperature, the magnetization becoming parallel to the *c*-axis. Neutron diffraction studies on YCo_5 revealed that this anisotropy can be attributed to the orbital contribution of Co magnetization [64]. Polarized neutron study on $NdCo_5$ showed that anisotropy mainly comes from site 2*c* [65].

RECo_5 compounds absorb hydrogen and their pressure-composition curves display multiplateau behavior corresponding to the formation of several hydride phases (α, β_I, β_{II} and γ) [66,67]. A maximum of 4.8 (1) H/f.u. has been found in the γ phase. Neutron diffraction studies on selected *RE*Co_5D_x compounds shows that the structure is preserved in the α phase [68]. β_I-$LaCo_5D_{3.35}$ and β_I-$PrCo_5D_{3.6}$ crystallize in an orthorhombic (*Cmmm*) structure with D atoms in RE_2Co_4 octahedral and RE_2Co_2 tetragonal sites. β_{II}-$PrCo_5D_{2.9}$ and β_{II}-$NdCo_5D_{2.8}$ crystallize in an orthorhombic body centered unit cell (*Im*2*m*), which is doubled along the *c* axis. β_{III}-$CeCo_5D_{2.55}$ crystallizes in a *C* centered orthorhombic structure with a doubling along *c*-axis (*Cccm* space group) with two partially occupied D sites. D insertion generates an anisotropic basal expansion, and a decrease of both Pr and Co moments.

In situ magnetic measurements under hydrogen pressure have been performed with a versatile vibrating-sample magnetometer connected to a pressure-composition measurement system [67]. It was used to measure the evolution of the magnetizations versus H content for several *A*Co_5 compounds (*A* = Y, La, Nd, Pr, Sm, Gd) between 77 and 420 K [66,67,69,70]. The comparison of the hydrogen pressure versus magnetization and hydrogen composition is displayed in Fig. 8 for $SmCo_5H_x$, clearly indicating that the magnetization decreases versus the H content. The magnetization decreases almost linearly versus H content for YCo_5H_x and $SmCo_5H_x$ hydrides [69,70]. This is attributed to the weakening of the Co-Co interactions by H insertion. In the case of $GdCo_5$, the total magnetization first decreases in the α-phase and then increases again, when the magnetization of Gd becomes larger than that of Co. Their Curie temperature decreases from 978 to 460 K for *A*=Y and from 953 to 480 K for *A*=Gd.

Herbst and Krönmuller [71,72] measured the magnetic aftereffect of the initial susceptibility in *RE*Co_5 deuterides (*RE*=La, Pr, Nd, Sm). The magnetic aftereffect is related to the interaction energy between the spontaneous magnetization and the interstitial atoms. The interaction energy depends on the deformations induced by the H(D) atoms on interstitial sites. They concluded that the deuterium atoms were mainly located in the *RE* plane compared to Co plane, in contradiction with the analysis of ^{59}Co Nuclear Magnetic Resonance (NMR) experiments [73]. But this last result was also later contested in Ref. [74] as the ^{59}Co NMR spectra of "YCo_5" in Ref. [73] corresponds indeed to a mixture of YCo_5 and Y_2Co_{17}.

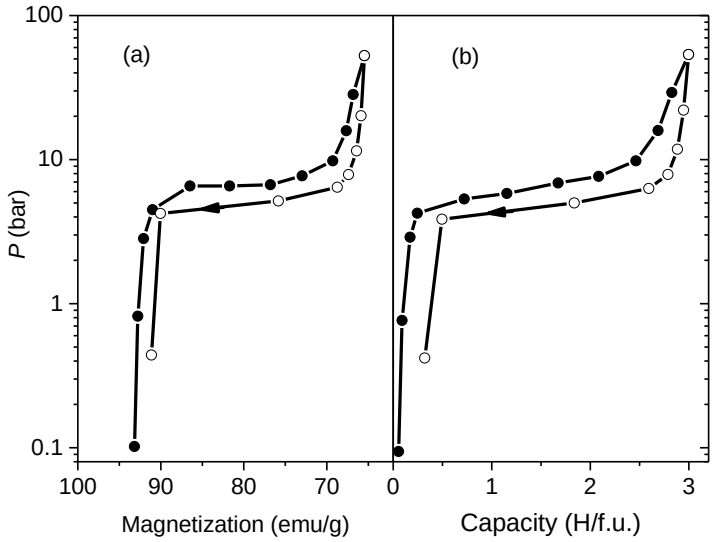

Fig. 8. Hydrogen pressure versus (a) saturation magnetization and (b) hydrogen composition in absorption (closed circles) and desorption (open circles) processes for the $SmCo_5H_x$ system at 25°C [69].

4.3 ANi_5 compounds

$LaNi_5$ is a Stoner-enhanced Pauli paramagnet with a magnetic susceptibility $\chi = 4.9\ 10^{-6}$ emu g^{-1} measured by NMR [75]. $LaNi_5H_{6.8}$ hydride displays a paramagnetic behavior with a slightly lower susceptibility with $\chi = 3.2\ 10^{-6}$ emu g^{-1} at room temperature. An *in situ* measurement in a Faraday balance connected to a microbalance measuring simultaneously the H pressure and concentration with the magnetic susceptibility [76] showed a correlation between the magnetization and the H content with a sharp magnetization decrease from α to β phase. First principles calculations of $LaNi_5$ predicted a weak ferromagnetic behavior due to the relatively high density of state at the Fermi level [77]. However further Density Functional Theory (DFT) calculations (with VASP) yielded to values lower than 1 for the Stoner exchange correlation integral: 0.78 and 0.94 for Ni sites 2*c* and 3*g* respectively [78]. This explains why the ground state is paramagnetic. The computed γ coefficient of the electronic specific heat γ = 23.12 mJ mol^{-1} K^{-1} [78], is smaller than the experimental one: γ = 34.5 mJ mol^{-1} K^{-1} [79] or γ= 42.6 mJ mol^{-1} K^{-1} [80]. The larger experimental values are explained by electron-phonon enhancement effects, which were not considered in the calculations.

The DFT calculations of $LaNi_5H_7$ indicated the presence of a metal-hydrogen state centered 5 eV below the Fermi level [77]. These calculations also indicate that the H atoms interact mainly with Ni, even if they have a better affinity with La atoms. The Fermi level is shifted to higher value due to the additional 7 e^- of H atoms and fall in the rising portion of the La atoms. However, the DOS at the Ni site is smaller than in the parent compound. As a consequence the magnetic susceptibility becomes smaller, despite γ decreases only slightly: γ= 40.4 mJ mol^{-1} K^{-1} for the $LaNi_5$ hydride [80] as the total DOS at E_F remains high.

Upon hydrogenation, $LaNi_5$ is reduced into fine powder, the grain size decreasing from 50 µm after 10 cycles to 12 µm after 100 cycles [81–83]. The magnetization curves show a ferromagnetic component due to surface segregation into Ni and La oxide. The ferromagnetic contribution increases also with the number of hydrogenation cycles, due to an increasing quantity of Ni nanoparticles. After 102 cycles about 1 % of Ni has been precipitated. *In situ* measurements of Blach *et al*. [76] confirmed the formation of Ni clusters upon cycling. Ni precipitation is also observed when $LaNi_5$ is exposed to air and this segregation can be attributed to the reaction of the surface of the alloy with traces of oxygen and water vapor. This self-restoring effect of the surface explains the easy activation and low sensitivity of $LaNi_5$ to impurities present in the hydrogen gas [83].

YNi_5 ($\chi = 23.10^{-4}$ emu $mole^{-1}$ at 4.2 K) and $CeNi_5$ are enhanced paramagnets with a broad maximum at 100 K for $CeNi_5$. $PrNi_5$ is a Van Vleck paramagnet with a peak around 16 K. Ferromagnetic behavior with low Curie temperatures was obtained for *A* = Nd (T_C = 6-8K), Sm (T_C = 27.5-41 K), Gd (T_C = 28-32 K), Tb (T_C = 23 K), Dy (T_C = 12 K), Ho (T_C = 4.1-4.5 K), Er (T_C = 8-10 K), Tm (T_C = 4.5 K) [51]. Magnetic measurements on single crystal revealed a large uniaxial anisotropy with generally a larger magnetization along the *c* axis [84]. Single crystal $DyNi_5$ is described in an ortho-hexagonal cell below T_C =11.6 K. In this description, *b* and *c* are respectively the easy and hard magnetization axes [85]. The spontaneous magnetization of 8.5 μ_B is mainly related to the Dy moment, but a small opposite moment of -0.08 μ_B/Ni is observed for Ni atoms.

The specific heats of $RENi_5$ compounds were measured to calculate the crystal-field splitting [86] as well as their magnetocaloric properties [87]. Both isothermal entropy and adiabatic temperature changes were measured and compared to calculated values using a Hamiltonian including crystalline electric field (CEF), exchange interaction and Zeeman effect. Rather good agreement was obtained considering that the experiments were performed on polycrystalline samples for *RE* = Er, Gd, Ho, Dy, Nd and Ce whereas the calculations assumed single crystal compounds. The influence of the easy axis orientation of the magnetization on the adiabatic temperature variation ΔT_{ad} was demonstrated theoretically for $ErNi_5$ [87]. The anomalous behavior of the entropy variation of $PrNi_5$ below 14 K was explained by the crossing of two fundamental CEF levels and by a sign inversion of the enthalpy and entropy variations compared to “normal case”.

4.4 $LaNi_{5-x}M_x$ compounds

The magnetic properties of $LaNi_{5-x}Fe_x$ compounds ($0 \leq x \leq 1.2$) have been studied by combining magnetic, transport and Mössbauer spectroscopy measurements [8,26,88–90]. For low Fe content ($x < 0.4$), a spin-glass behavior is observed at low temperature. It is separated from the paramagnetic range by an intermediate region of strong irreversibility. Above a critical concentration $x_C = 0.4$, a percolation threshold is observed as the density of substituted Fe atoms becomes enough to induce a ferromagnetic state coexisting with the freezing of small magnetic clusters below 15 K. The Curie temperature increases sharply from 45 to 300 K for $x = 0.4$ to 1.2 respectively. The larger total magnetization compared with the Fe moment measured by Mössbauer spectroscopy at 4.2 K (m_{Fe} =1.52 μ_B) shows that the Fe substitution induces a Ni moment m_{Ni} of 0.62 μ_B. In addition, X-ray diffraction measurements under applied field indicated that the easy magnetization axis is oriented along the *c* axis for $x = 1.2$. Similar but less pronounced effect was found for x =1.0. These compounds can absorb hydrogen concentration between 5.9 H/f.u. for $x = 0.25$ to 5.4 H/f.u. for $x = 1$. The neutron diffraction study of $LaNi_4FeD_{5.1}$ reveals that the $CaCu_5$ structure is preserved with a cell volume expansion of 16% and D atoms distributed over three interstitial sites [26]. The magnetic curves of $LaNi_{5-x}Fe_xH_y$ hydrides indicate that the magnetizations are weak, and that they increase with Fe concentration. Hydrogenation enhances the spin-glass character and favors a transfer of *d* electrons towards H atoms as observed through the decrease of the isomer shift measured by Mössbauer spectroscopy.

The influence of the partial substitution of Ni by *M* = Co, Cu, Fe, Mn and Al on the electronic properties of $LaNi_4M$ compounds was studied by X ray absorption and photoemission in comparison with band structure calculations [91]. It shows the presence of a new band which is full and below the Ni *d*-band for Al (E_F-E = -6 eV) and Cu (E_F-E = -3 eV) and crossing the Fermi level for Mn, Fe and Co. The influence of multi-substitution (Mn, Al, Co) was investigated in view to study properties of battery materials.

5. Electrochemical applications of $LaNi_5$-type hydrides as anodes in Ni-*M*H batteries

Beside hydrogen gas storage, metallic alloys (*M*) can be considered as suitable materials for electrochemical energy storage. Indeed, the reaction between *M* and hydrogen can follow either a solid-gas or an electrochemical route, according to the two equivalent reactions (1) (driving force P_{H_2}; equilibrium pressure) and (2) (driving force E_{M/MH_x}; equilibrium potential):

$$M + \frac{x}{2}H_2 \leftrightarrow MH_x \qquad (P_{H_2}) \qquad (1)$$

$$M + xH_2O + xe^- \leftrightarrow MH_x + xOH^- \qquad (E_{M/MH_x}) \qquad (2)$$

However, for practical use, the reversible hydride formation reaction should take place at low pressure (typically between 1 and 0.01 bar), near-ambient temperature range (-20 to 40°C) and alkaline medium. Metal-hydride couples fulfilling these conditions would then be suitable to work as anodes in alkaline batteries.

The market for these alkaline systems took off with a patent filed in 1899 by Waldmar Jungner [92], which marks the invention of the nickel-cadmium (Ni-Cad) accumulator, founding a company that will later become SAFT AB. These accumulators consist of a positive nickel hydroxide electrode and a negative cadmium electrode immersed in a concentrated KOH solution. They are still used today for emergency lighting units (ELU), backup applications and uninterruptible power supplies (UPS). They are however limited in terms of energy density, poorly eco-friendly because of cadmium and subjected to internal drying as the electrochemical operating reactions consume water.

For the above reasons, research works were conducted in the sixties to improve energy density and service life of these batteries. In 1967, a first attempt was made in Geneva with an anode using a titanium-nickel based alloy [93] capable of reversibly storing hydrogen in front of the positive nickel hydroxide-based electrode: the first Ni-*M*H battery was born. The main advantage of this battery is that, keeping both the alkaline electrolyte and the positive nickel hydroxide cathode developed for Ni-Cad batteries, one produces a striking gain in volume energy (from 120 $Wh.L^{-1}$ for Ni-Cad to 240 $Wh.L^{-1}$ for Ni-*M*H). Moreover, the alternative to cadmium, toxic to the environment, was also a significant benefit. Finally, the charge-discharge electrochemical reactions of the Ni-*M*H battery do not involve water so that the water content remains constant in the cell over the whole cycle, unlike those

involved in Ni-Cad batteries. This strongly facilitates the development of industrial devices and explains the rapid introduction of Ni-*M*H systems to the market, as early as 1989, notably by Japanese companies such as Sony, Yuasa, Panasonic (formerly Matsushita), Toshiba and Sanyo.

Though a Ti-Ni based metal hydride was first considered in the early days, this alloy was rather unstable and inappropriate for industrial developments. However, following this idea, research continued, notably at Philips laboratories in the Netherlands and CNRS in Meudon (France). In 1970, the alloy $LaNi_5$, able to store more than 6 H/f.u. by the solid-gas route was discovered, rapidly tested as a negative electrode [94–97] in alkaline medium and patented in 1975. The binary alloy is however subject to rapid corrosion, and many studies were then performed to stabilize the intermetallic in alkaline medium [98–103].

First, the plateau pressure of $LaNi_5$ reaches 1.7 bar at room temperature. As a result, the binary compound is not suitable as an anode in open batteries since its hydride ($LaNi_5H_6$) will decompose spontaneously under normal conditions of pressure and temperature. To solve this, as we have seen in Sections 2 and 3, nickel can be partially substituted by elements with large atomic radius to lower the plateau pressure in the suitable range of 0.01 to 1 bar. As an example, the potential versus time evolution of a $La(Ni,Al,Mn,Co)_5$-type negative electrode during a galvanostatic cycle is shown in Fig. 9 in a half cell [37]. During charge at *C*/10, one observes a potential plateau at -950 mV *vs.* ENH reference electrode. This potential plateau is the electrochemical equivalent to the pressure plateau for the solid-gas reaction, following the metal-hydride phase transformation. The plateau extends for about 10 hours before showing a small kink related to hydrogen evolution at the electrode surface when the charge is over (*i.e.* after full formation of the metal hydride phase). For discharge, one sees a sloped potential plateau ranging between -900 and -630 mV *vs.* ENH for the same duration (10 h), which reflects the complete restitution of the inserted hydrogen. The difference between charge and discharge potentials is mainly related to kinetic limitations in the charge transfer at the electrode surface and to the diffusion of hydrogen atoms within the storage material. Indeed, $LaNi_5$-type compounds are known to have very fast bulk reaction kinetics. At the surface, this is ensured by the spontaneous formation of nanoparticles of metallic nickel, which are highly active in the decomposition of water due to the corrosion of the compound in alkaline medium. At the volume level, the diffusion of hydrogen in the intermetallic compound at room temperature is very high ($2\ 10^{-8}$ cm^2/s) [104], allowing the hydrogen atoms to travel at a speed of about 10 µm/min in the material.

Such half-cell illustrates well the behavior of *M*H anodes but differs from real mechanisms taking place in commercial Ni-*M*H cells. In real batteries, the cathode is the limited electrode so that side reactions always take place at the positive electrode, releasing oxygen when overcharged and hydrogen when over-discharged. These gas evolvements must be avoided to prevent any pressure increase in a sealed accumulator. The over-capacitive anode compensates by allowing recombination reactions of the gas as the oxygen produced at the positive electrode is recombined by reaction with the hydride at the negative electrode. In a similar way, at the end of the discharge, the hydrogen produced at the positive electrode reacts by solid-gas reaction with the metal of the negative electrode to form the hydride. Thanks to these recombination reactions, it is possible to limit any gas evolution, pressure rise and electrolyte leakage.

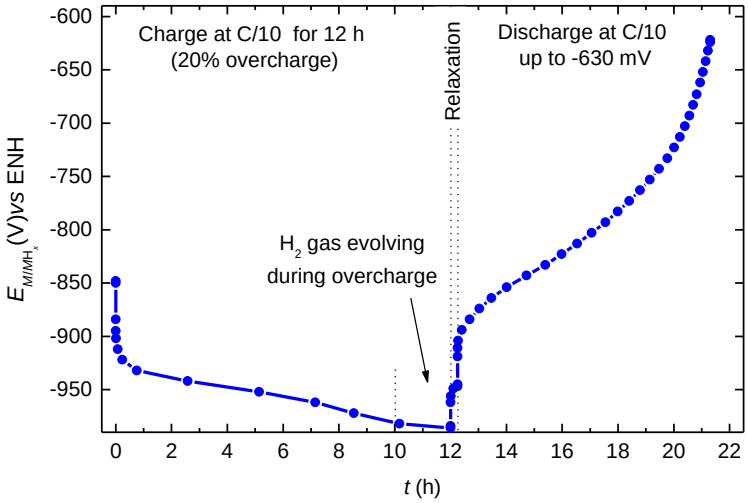

Fig. 9. Typical galvanostatic charge-discharge cycle for a $LaNi_5$-type *M*/*M*H_x electrode studied in half -cell in KOH 8N electrolyte. Charge rate at *C*/10 for 12 h (20% overcharge) and discharge rate at C/10 up to -630 mV versus ENH reference electrode. The alloy *M* forms the hydride *M*H_x during charging up to 10 h, then gas evolution is observed during overcharge. After a short relaxation period, the hydride releases reversibly hydrogen during discharge for 10 h with increasing potential up to -630 mV. *[37]* Cambridge University Press, Copyright Clearance Center; License Number 4910200018114.

In addition to adjusting the plateau potential (*i.e.* pressure), the optimization of the performance of $LaNi_5$-derived compounds for Ni-*M*H batteries focused on reducing the cost of the alloy and improving their lifetime. As a result, and taking full advantage of substitution effects, commercial $LaNi_5$-type alloys have nowadays very complex formulation. A typical composition of the active material constituting these anodes is *Mm*$Ni_{3.55}Mn_{0.4}Al_{0.3}Co_{0.75}$, first proposed in Ref. [105].

The use of Mischmetal (*Mm*, a mixture of rare earths which composition depends on the ore) is first based on economic criteria because rare earth separation processes, which have similar chemical properties, are quite expensive. However, contribution of cerium in La-rich *Mm* brings also an interesting effect related to the change of its valence state and therefore size upon hydrogen absorption. *In situ* hydrogen loading studies using X-ray absorption (XAS) have been performed on $La_{1-x}Ce_xNi_{3.55}Mn_{0.4}Al_{0.3}Co_{0.75}$ [106]. The Ce valence, which is around 3.35 in the alloys, slightly decreases in the α phase and sharply in the β one, reaching 3.1 above 5 H/f.u., *i.e.* close to a trivalent state. With respect to the triple substitution of Ni, the lowering of the plateau pressure is achieved by the incorporation of Mn and Al, while the choice of cobalt is driven by lifetime considerations. Interestingly, hydrogen absorption modifies also the K-edge of the transition metals: the intensity of the 1*s*-3*d* pre-peak decreases with H loading.

From the very first studies of the electrochemical properties of the binary compound $LaNi_5$, it was noted that, during electrochemical cycling, the reversible capacity decreases by half in less than 100 cycles [97]. Decrepitation of the alloy, resulting from the high mechanical stresses generated by the difference in volume between the metal and hydride phases (up to 30%), is at the origin of this short service life. Consequently, the generation of new fresh surfaces accelerates the corrosion of the alloy in the alkaline medium by reducing the quantity of active material to the benefit of the formation of *RE* hydroxides and a nanoporous Ni surface layer [107]. In addition, decrepitation can cause loss of electrical contacts between the active material and the electron conducting network. Cobalt substitution has proven to be a very good solution to cope with the phenomena of decrepitation. Cobalt leads to the formation of a second hydride phase with a concentration between 3 and 3.5 H/f.u., *i.e.* about half of the full capacity. This intermediate hydride enables the hydrogenation process to be separated into two stages, each resulting in smaller volume variations. This reduces the mechanical stresses within the material during hydrogen insertion/disinsertion and thus reduces its decrepitation.

The multi-substituted alloys *Mm*(Ni,Mn,Al,Co)$_5$ present the best compromise between capacity and service life with values close to 300 mAh/g over several hundred cycles. This was attributed again to the peculiar role of cobalt as, for this composition, *in situ* neutron analysis during electrochemical cycling revealed the formation of an unexpected intermediate γ phase existing in equilibrium with both the α and β ones [108]. The γ phase has an average cell volume (97 to 98 Å^3) between those of α and β. It plays a key role in the strain distribution within the crystal structure. This can be understood in term of volume expansion upon hydrogenation, responsible for severe grain pulverization, creating fresh surfaces in contact with the electrolyte, and inducing enhanced corrosion. The existence of γ at the interface between α and β, mitigates the cell volume increase attributed to the sole α to β expansion as it implies a two-step mechanism for the discrete volume expansion (α to γ, then γ to β) thus reducing the crystal strains and limiting the decrepitation. However, cobalt remains an expensive critical raw material (10 wt.% of cobalt represents about 40% of the cost of the material) and its content must be controlled. The use of over stoichiometric compounds *Mm*(Ni,Mn,Al,Co)$_{5+\delta}$, for which the volume changes of the crystallographic lattice during the metal/hydride transition are reduced, has been proposed [109]. This alternative has made possible a significant reduction of the cobalt content in multi-substituted alloys, and even to get rid of it by subsequent Fe substitution [110–112].

Beside the fine composition optimization of these $LaNi_5$-based anode materials, valuable efforts have been made to understand their behavior along electrochemical cycling. Magnetic measurements have been used to study their evolution under corrosion and after cycling. Broom *et al*. [113] studied La*Mm*Ni$_{3.43}$Mn$_{0.38}$Al$_{0.29}$Co$_{0.67}$ together with a surface treated modified alloy, to enhance Ni formation at the surface. The uncycled sample is paramagnetic with χ= 0.179 emu/g. The surface treated modified alloy displays a spontaneous magnetization suggesting the presence of Ni nanoparticles due to the surface treatment. The magnetization increases upon cycling due to superparamagnetic particles clustering at the surface of the grains. The analysis of the *M*(*B*) curves with a Langevin equation gives an average Ni cluster size of 5200 atoms. In addition, thermomagnetic measurements show that T_C is higher than that of pure Ni suggesting a Ni-Co alloying effect.

Electrochemical properties of $LaNi_{3.55}Mn_{0.4}Al_{0.3}Co_{0.75-x}Fe_x$ ($0 \le x \le 0.75$) compounds were also studied [114–116]. The evolution of their magnetic properties was used to characterize the sample corrosion and explain the capacity decrease versus the number of electrochemical cycles (10, 20 and 50 cycles), more pronounced for x = 0.75. The analysis of the *M*(*T*) curves was used to quantify the percentage of decomposed alloys upon cycling, which increases with the Fe concentration and the cycle number. The variation of the Curie temperatures allowed to determine the chemical composition of the segregated particles using Ni(Co,Fe) alloys as references. The nano-particles were identified as Ni(Co,Fe) alloys, but with a larger Ni concentration compared to the initial stoichiometry. The average nanoparticle size was measured thanks to the Langevin equation. Their diameters were found between 3 to 12 nm, with a maximum after 10 cycles. The magnetic data were also used to estimate the percentage of hydroxide which reaches 16 % after 50 cycles for x=0.75. An estimation of the corrosion layer thickness was also made. It increases linearly with the number of cycles and the slope is proportional to the initial Fe concentration. These results were correlated to the larger electrochemical capacity diminution when all the Co atoms are replaced by Fe and explained by a larger corrosion effect.

About thirty years of research were necessary to optimize the composition of $LaNi_5$-type alloys as negative electrode materials for Ni-*M*H batteries [117]. The binary compound $LaNi_5$, at the basis of the concept, thus became over-stoichiometric and multi-elemental, comprising up to nine different metals. The adaptation of the alloy formulation needed at least three decades of research to define the best compromise in terms of electrochemical stability, capacity, lifetime and cost. This explains the commercial success of these batteries since the 1990s that are now sold by millions of units for Hybrid Electric Vehicles or Emergency Light Units.

Nowadays, the story is still ongoing with the development of new alloys able to further improve electrochemical capacities while controlling the lifetime and cost. This can be achieved by developing a new generation of anode materials based on (A,Mg)$_2$B$_7$ or (A,Mg)$_5$B$_{19}$ inter-growth structures (*A*: *RE*) [118]. These new phases are formed from [AB_5] and [A_2B_4] layers, stacked alternatively along the *c*-axis. The chemical formula of this type of alloys can be expressed as $n[AB_5]+m[A_2B_4]$, *i.e.* ($A_{n+2m}B_{5n+4m}$), where *m* and *n* represent the integer numbers of the successive layers. Each of these phases might adopt two types of crystallographic structure: hexagonal ($P6_3mc$) and rhombohedral (R-3m). AB_2 alloys (layer [A_2B_4]) are known to provide a high hydrogen absorption capacity but limited

stability, while AB_5 type alloys are widely used in alkaline batteries with a remarkable lifetime but a lower capacity. Since A_2B_7 and A_5B_{19} alloys are made by combining stacked layers of [A_2B_4] and [AB_5], a higher capacity than pure AB_5-type alloys can be achieved, together with a better lifetime than AB_2 ones [119]. Indeed, pseudo-binary alloys of the $(A,Mg)_2B_7$ and $(A,Mg)_5B_{19}$-type absorb hydrogen reversibly with one flat single plateau and similar atomic capacity to the binaries, which is excellent for electrochemical application [120–123]. Moreover, substitution by Mg, allowed in the [A_2B_4] layer, leads to reduce molar mass of the compounds, thus increasing the weight capacity of the alloys. It has been suggested that, in these systems, the [AB_5] layers act as hydrogenation catalyzers of [A_2B_4] ones [124].

6. Non-electrochemical applications of AB_5 compounds

The most successful application of metal hydrides, and in particular of AB_5-compounds, is undoubtedly their use as negative electrodes of Ni-*M*H batteries. Principles of electrochemical hydrogen storage and optimization of AB_5 alloys for this application have been discussed in the previous section. Here, we will focus on applications involving the solid-gas reaction with special attention to those for which AB_5 alloys are best adapted.

Practical applications of interstitial metal hydrides are essentially driven by the reversibility of hydrogen uptake/release between metal and hydride phases and the possibility to tune the reaction as a function of pressure and temperature [125,126]. The reversibility of the solid-gas reaction, which is accompanied by heat exchange, can be expressed as:

$$M(s) + \frac{x}{2}H_2(g) \leftrightarrow MH_x(s) + heat \qquad (3)$$

while the thermodynamic properties of the reversible reaction, *i.e.* the dependence of the plateau pressure P_p with the temperature T, are given by the van't Hoff relation:

$$ln\frac{P_p}{P_o} = \frac{\Delta H}{RT} - \frac{\Delta S}{R} \qquad (4)$$

where P_o is the reference pressure (usually 1 atm), ΔH and ΔS are the enthalpy and entropy changes of the phase transformation, respectively, and R is the gas constant. Characteristic data for $LaNi_5$ are $x \sim 6.5$ (H/f.u.) *i.e.* 1.5 wt% and 105 kgH_2/m^3, P_p = 1.7 atm at 298 K, ΔH = -31 $kJ/molH_2$ and ΔS = -110 $J/K\ molH_2$ [39].

The choice of AB_5 compounds for a given application is guided by their advantages and constrained by their shortcomings [127]. $LaNi_5$-type alloys are characterized by their versatile thermodynamic properties enabled by substitutional effects, high volumetric capacity, easy activation, a unique flat plateau with moderate hysteresis, rapid kinetics, resistance to poisoning and good cycle stability. As drawbacks, they have moderate gravimetric capacity, decrepitate to very fine powder and contain expensively and unevenly distributed elements in the earth, *i.e.* rare earth metals that are considered as critical raw materials in most countries.

Besides electrochemical storage, main applications of $LaNi_5$-type compounds can be classified in three families (Fig. 10): solid-gas hydrogen storage, thermally powered devices and gas separation.

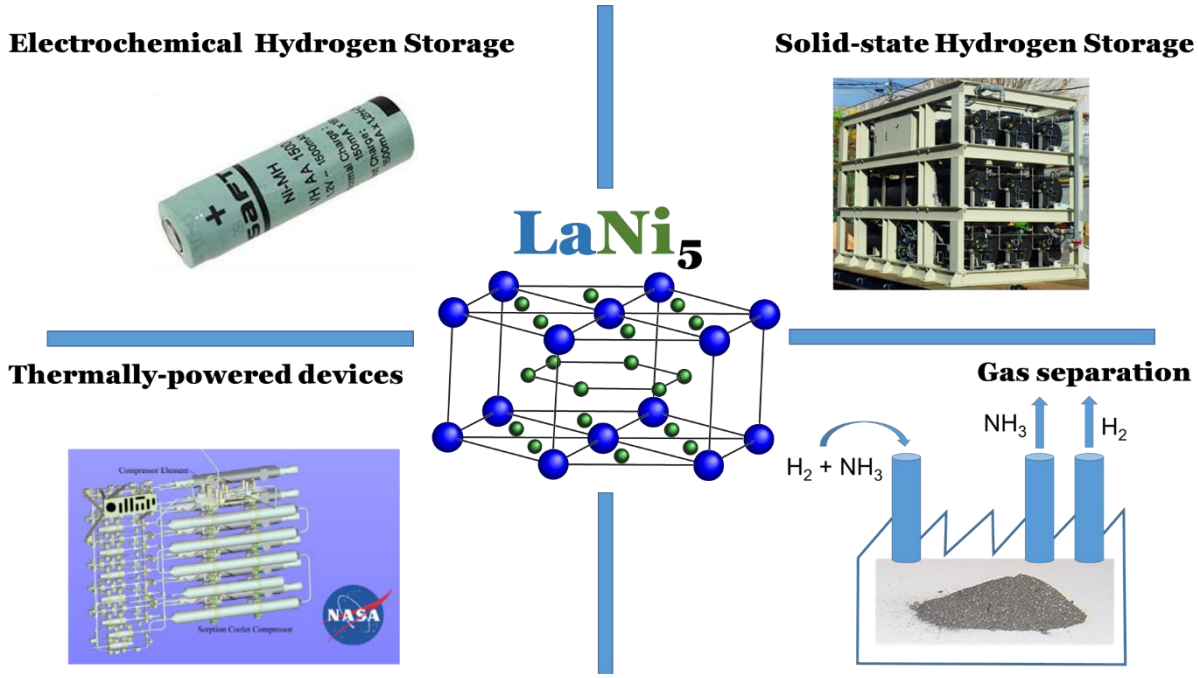

Fig. 10. Main applications of $LaNi_5$-type compounds. Images for Solid-stage Hydrogen Storage and Thermally-powered devices taken from Ref. [128] and [129], respectively.

6.1. Solid-state hydrogen storage

Following the discovery of the remarkable properties of $LaNi_5$ alloy as reversible hydrogen store [95], its use in commercial devices for hydrogen storage has been attempted by many companies worldwide during the last 50 years [130–136]. $LaNi_5$-derivatives have been used in portable, mobile and stationary applications. Some examples of portable applications are smartphones [137], personal power sources [138] and minibar coffee machines [139]. As for mobile applications, bikes [140], utility vehicles [126] and forklifts [141] have been developed. The use of AB_5 compounds for these applications is generally driven by their high volumetric energy density and mild operating conditions (safety). However, their widespread commercialization is hampered by weight penalty and cost-issues as compared to alternative power sources, mainly batteries. Forklifts, which require ballast for stability, are foreseen as an exception to this general statement. Fuel-cell powered forklifts are characterized by lower costs of operation, shorter refueling time and less maintenance than battery powered forklifts [141].

Most of both portable and mobile applications using metal hydrides concern prototypes or few units for niche demands. The low gravimetric energy density of metallic hydrides and the need for heat exchange to promote reversible hydrogen sorption account for this. These drawbacks of metal hydrides are less constraining for stationary applications in which the ratio of the heat exchanger counterpart to the balance-of-plant can be minimized and waste heat used. In particular, the use of room-temperature metal hydrides has recently gained a vivid interest as concerns the energy management of intermittent renewable energies [142,143]. For instance, a prototype tank containing 29 kg of $LaNi_{4.8}Al_{0.2}$ has been tested in Europe to deliver hydrogen to a PEM fuel cell at 1.5 bar and 2.6 Nl/min flow, while using a water heating system to maintain desorption temperature at 333 K [144]. In Japan, AB_5 alloys have been recently used in much larger storage devices by Toshiba corporation and the Japan Steel Works (JSW) as now detailed.

The H2One™ modular system developed by Toshiba corporation aims to produce hydrogen by electrolysis using renewable energy, store the produced hydrogen in a metal hydride tank, and convert it into electricity using a fuel cell when needed [145]. It has been used, for instance, to manage electricity for a Hotel resort in Japan using photovoltaic panels as a primary source. The metal-hydride AB_5 tank is loaded in summertime with the surplus of electricity production and unloaded in wintertime to feed-up a fuel cell. This fuel cell not only guarantees stable electricity production but also provides heat and warm up water for the Hotel resort. The *M*H tank is less than one-tenth of the size of the conventional type gas tank it replaces and can store 200 Nm^3 (18 kg) of hydrogen. JSW company has

developed even larger *M*H-tanks based on AB_5 alloys with composition $MmNi_{4.4}Mn_{0.1}Co_{0.5}$, being first prototype developed for the renewable energy system constructed at Griffith University, Australia [128,131]. The alloy powder, with a typical particle size of 1 mm, is embedded in a special resin that permits hydrogen permeation. This composite material ensures uniform distribution of alloy in the tank and reduces mechanical stress. The whole system works near ambient conditions of pressure and temperature. It is composed of 9 metal hydride tanks with a total capacity of ~ 90 kgH_2 (1000 Nm^3).

6.2 Thermally powered devices

The operation of hydride-based thermodynamic devices relies on the large pressure response of hydrides to changes in temperature (Eq. 4), on the heat exchange during hydrogen sorption (Eq. 3), or both. Compared to other mechanical and chemical systems, hydride-based thermodynamic devices have unique properties: use of a non-polluting working fluid (hydrogen), lack of moving parts, compactness, fast response with proper heat management, and low cycle time. Most successful thermally-driven devices using AB_5 compounds are compressors, actuators, sensors and heat chemical engines.

Thermal energy can be converted into the compression of hydrogen when a hydride bed is heated up in a closed volume. According to the van't Hoff relation, hydrogen pressure increases with temperature. For $LaNi_5$, the plateau pressure increases from 2 to 49 bar when rising the temperature from 298 to 400 K. In practical devices, several hydride beds can be assembled in series to enhance the compression ratio. For two consecutive beds, the plateau pressure of the first bed at high temperature should be higher than that of the second bed at low temperature. As early as in 1973, a three-stage hydrogen compressor using $LaNi_5$ was built-up by van Mal *et al.* following this concept. Hydrogen was compressed from 4 to 45 bar while the temperature was ranged between 290 and 410 K [146]. The total cycle time was 10 min with a hydrogen flow of 15 mg H_2/s.

One of the most successful applications of hydride-powered compressors are sorption cryocoolers for refrigeration of telescopes in spacecrafts. These cooling devices combine a thermal compressor system, to rise hydrogen pressure, and a Joule-Thompson expander to cool down hydrogen at cryogenic temperatures [126,146]. The Brilliant Eyes Ten-Kelvin Sorption Cryocooler Experiment (BETSCE) developed by the Jet Propulsion Laboratory (JPL-USA) and launched in 1996 demonstrated highly efficient cooling down to 10 K [147,148]. Compressor beds contained a $LaNi_5$-type alloy able to compress hydrogen from 0.7 to 100 bar for a temperature swing comprised between 270 and 470 K. This device could perform thousands of thermodynamic cycles without losing performance. This was achieved thanks to partial Ni by Sn substitution in $LaNi_5$ alloy ($LaNi_{4.8}Sn_{0.2}$) for minimizing alloy degradation on cycling. Research works showed that Sn substitution promotes a more homogenous distribution of hydrogen atoms in the alloy as compared to $LaNi_5$ [149]. Thus, strain gradient and dislocation generation are minimized leading to less microstructural damage than for binary $LaNi_5$. Similar engineering and metallurgical approaches were latter used for a double sorption cooler used in the Planck Surveyor mission of the European Space Agency launched in 2009 [129].

Nowadays, much activity of hydrogen compressors is motivated by the need of pure hydrogen supply at high-pressures for refueling hydrogen vehicles (cars, buses, forklifts…). Recently, several comprehensive review papers on this topic have been published [150–152]. Most compressor systems operate at mild temperatures (between room temperature and 425 K) to use low-grade waste heat (T < 200 °C) from electrolyzers, fuel cells and so on… For instance, in refueling stations, on-site hydrogen production by electrolyzers can be envisaged and the generated low-grade heat used for powering hydrogen compression [153,154]. To produce high hydrogen pressures (P_{H2} > 200 bar), multi-stage compressors are required. In these systems, AB_5 compounds are preferred for initial stages since, at low and moderate pressure (P_{H2} < 200 bar), they have flat plateau, reduced hysteresis, fast kinetics and good resistance to impurities. The latter property is of paramount importance for the first stage of the compressor (see Section 6.3). Plateau slope and hysteresis play a key role on the compression ratio, whereas kinetics largely determine the productivity of the system. Tailoring of thermodynamic properties of $LaNi_5$-derived compounds entailed the partial substitution of La by Ce or *Mm* for hydride destabilization and the partial substitution of Ni by Co, Mn, Al and Sn for hydride stabilization, hysteresis control and cycle-life enhancement. For instance, $La_{0.5}Ce_{0.5}Ni_5$ compound has been developed by the group of Lototskyy for the first stage of a 200 bar compressor [150,151].

The increase of hydrogen pressure with temperature induced by hydride thermal desorption in a closed system can also be employed to operate actuators and sensor devices. In actuators, changes in hydrogen pressure are converted into mechanical movement. As an example, Kurosaki *et al.* used 10 g of $LaNi_5$ to lift 20 kg load with a displacement of 8 cm [155]. The sorption bed was increased from 270 to 350 K with a concomitant pressure increase from 4 to 8 bar. This concept has been applied with success using $LaNi_5$-type alloys in rehabilitation therapy, human power assistance and robotics [156,157].

As concerns sensor, pressure changes in a closed volume by heat-driven hydrogen desorption can be calibrated and used, for instance, to move a fluid control valve [125]. This has been used by the company Ergenics for fire detection and activation of a sprinkler head valve when the temperature reaches a predetermined temperature. According to patent data, approximately 4 g of a $LaNi_5$-compound are placed in the sensor to achieve upon thermal desorption hydrogen pressures of about 6 bar [158]. The temperature response of this sensor-actuator can be tuned by partial substitution of Ni by Fe, Co, Al or Sn in $LaNi_5$ alloy. The sensor is fully reversible and stops fluid release once the temperature goes back to ambient.

Heat chemical engines such as heat pumps, for heating, and refrigeration devices, for cooling, manage heat exchange during hydrogen sorption (Eq. 3). Heat pumps exploit the heat released by hydrides during absorption while refrigeration devices use the ability of hydrides to uptake heat for desorbing. In both devices, hydrogen gas is transferred between two hydride reservoirs at two different temperatures. Multi-stage systems containing up to 16 different metal hydride beds have been implemented in the literature [159]. Operation details are given in excellent book chapters and review articles on this topic [125,160,161].

AB_5 compounds have been widely used in heat chemical engines [159,161]. For instance, Gopal and Murphy implemented a cooling system in which $MmNi_{4.5}Al_{0.5}$ was used as high pressure – low temperature alloy, releasing heat out of the system when hydrogen was transferred to a low pressure – high temperature alloy [162]. The working temperature of the AB_5 alloy was set between 278 and 303 K. In contrast, Sekhar and Muthumar demonstrated the feasibility of a double-stage system to upgrade heat from 393 to 463 K using $La_{0.35}Ce_{0.45}Ca_{0.2}Ni_{4.95}Al_{0.05}$/ $LaNi_5$/$LaNi_{4.35}Al_{0.65}$ alloy combination [163].

6.3. Gas separation

Gas separation devices are based on the selectiveness of some metals and intermetallic compounds to react reversibly and exclusively with hydrogen (Eq. 3). As remarked by Dantzer [161], one should distinguish between separation and purification processes. The latter term only applies to separation of hydrogen from other gases when the level of impurities is below 0.1 %. Separation processes using metal hydrides are particularly relevant when hydrogen is mixed with low or inert reacting gases such as Ar, He, N_2, CH_4 and NH_3. Reactive gases such as O_2, CO_2 and CO are difficult to separate from hydrogen using metallic hydrides, though successful results in AB_5 compounds have been achieved by surface modification with fluorination treatment or Pd coatings [164]. Particularly, carbon monoxide is considered as a poison for hydrogen absorption in metals [165,166].

$LaNi_5$-type compounds are particularly adapted for the separation task thanks to their endurance towards poisoning compared to other intermetallics and reversible hydrogen uptake [166–168]. In a hydride bed, the alloy reacts reversibly only with hydrogen from the gas mixture to form the hydride. Inert impurity gases remain in the volume of the container, while reactive ones are irreversibly chemisorbed at the AB_5 surface. After a venting step to flush inert gases, pure hydrogen can be recovered from the hydride bed. The concept has been applied, for instance, in large-scale systems using a $MmNi_{5-x}Al_x$ alloy to separate hydrogen obtained as a by-product of a synthetic ammonia plant [169]. Hydrogen separation from ammonia using $LaNi_5$ has also been demonstrated from the argon vent stream of an ammonia synthesis loop [170]. Starting with an initial hydrogen content of 60%, the hydrogen purity reached up to 99.9%.

Metal hydrides can be also used for the separation of hydrogen isotopes (protium, deuterium and tritium). Several H-sorption properties of metals such as thermodynamics, diffusion coefficients and

kinetics depend on the isotope [171]. As for thermodynamics, the plateau pressure of a given metal-hydrogen system depends on the nature of the isotope. Thus, the efficiency of the separation between two isotopes by thermodynamic means can be evaluated by the separation factor, which for a mixture of hydrogen and deuterium gases is given by:

$$\alpha_H^D = \frac{(\frac{D}{H})_{gas}}{(\frac{D}{H})_{solid}} \quad (5)$$

where D and H represent the concentration of the isotopes in gas and solid phases.

Isotopic dependence in intermetallic compounds is complex. $LaNi_5$-type compounds are a good example of this statement. Early works of Percheron-Guégan *et al.* in 1977 showed that the separation factor between deuterium and hydrogen in Ti-substituted $LaNi_5$ between 233 and 283 K is low (α < 1.33) and tends to 1 when the temperature approaches to the ambient [172]. This means that isotope effects are small in $LaNi_5$. This was confirmed by Andreyev *et al.* [173] both for deuterium and tritium as well as by Yawny *et al.* [174] who concluded in 1989 that $LaNi_5$ is not adequate for isotope separation purposes. However, the same year Sakaguchi *et al.* [175] disputed this affirmation by showing that $LaNi_5$ thin films deposited over polyimide membranes can reach a high separation factor (α = 1.9) in the range 353-423 K, comparable to Pd films. This significant enhancement was mainly attributed to the difference of diffusivity between hydrogen and deuterium in $LaNi_5$. More recently, in 2006, it has been reported that magnetization effects can also influence the isotope separation for ferromagnetic $LaNi_5$-type alloys [176]. Indeed, for $LaCo_5$ compound the separation factor at the high-pressure plateau increased from 1.54, at zero field, up to 2.25 at 13 T.

To summarize, $LaNi_5$-type compounds are highly versatile systems for reversible hydrogen sorption near room temperature and pressure. Their H-thermodynamic properties can be tailored at wish through chemical substitution for being adapted to the operation conditions of multiple applications of high technological interest. To illustrate this fact, Table 2 gathers representative $LaNi_5$-type compounds used for the main applications described in this Section.

Table 2
Representative $LaNi_5$-type compounds used in successful applications other than Ni-*M*H batteries

Application	Alloy Composition	Temperature range (K)	Pressure range (bar)	Reference
H-storage stationary	*Mm*$Ni_{4.4}Mn_{0.1}Co_{0.5}$	298-308	1-8	[128]
H-storage stationary	$LaNi_{4.8}Al_{0.2}$	335	1.5	[144]
H-storage portable	*Mm(*Ni,Mn,Co)$_5$	273-315	1-10	[137]
H-storage mobile	$La_{0.6}Ce_{0.4}Ni_5$	293-338	2.5-30	[138]
Compression	$LaNi_5$	298-333	5-13	[153]
Compression	$La_{0.5}Ce_{0.5}Ni_5$	288-413	1-70	[150]
Compression	$LaNi_5$	290-410	4-45	[146]
Cryocooling	$LaNi_{4.8}Sn_{0.2}$	270-470	0.7-100	[147,148]
Cooling system	*Mm*$Ni_{4.5}Al_{0.5}$	278-303	-	[162]
Actuator	$LaNi_5$	270-350	4-8	[155]
Heat sensor/actuator	La(Ni,Fe,Co,Al,Sn)$_5$	298-408	2-7	[158]
Gas separation	*Mm*$Ni_{5-x}Al_x$	300	-	[169]
Gas separation	$LaNi_{3.55}Co_{0.75}Mn_{0.3}Al_{0.4}$	350-475	0.1-8	[166]
Purification	$LaNi_{4.3}Al_{0.7}$	298-355	8	[168]

7. Conclusion

In this review, the most outstanding properties of AB_5 compounds have been presented. $LaNi_5$-derived compounds crystallize in the hexagonal $CaCu_5$-type structure. This structure, though rather simple can accommodate many substituting elements in large amounts, allowing to modify at wish and to a large extent the compound properties. Such compounds can absorb reversibly large quantity of hydrogen, which is of extreme importance for various applications such as Ni-*M*H batteries, stationary hydrogen tank, compression, cryocooling, gas separation or purification. The large substitution range aforementioned allows to finely adjust the thermodynamic properties to fulfill the desired application. The magnetic properties of *RE*Co_5 and *RE*Ni_5 compounds can be also modified by combining chemical substitution and hydrogen absorption. The *LRE*Co_5 compounds have been extensively studied for permanent magnet application, particularly $SmCo_5$. Magnetic measurements have been also used to study the surface decomposition either in solid gas or in electrochemical condition due to oxidation or corrosion effects, respectively. The concept of composition adjustment has been particularly developed for Ni-*M*H battery, defining very accurately $LaNi_5$-type anode materials and leading to the most successful commercial application so far for metallic hydrides. Research on this family is no longer as active as in the 90's. However, exploration is still running on new families of super-lattice alloys, all built from $LaNi_5$-based units showing the great versatility of this compound for energy storage applications. Significant research programs are nowadays conducted worldwide for both stationary and mobile energy storage usages. This review highlights the extraordinary chemical flexibility of AB_5 compounds and its use on manifold applications over the last 50 years. This compound family remains today of vivid interest face to current challenges on energy storage technologies.

References

[1] E. Burzo, Hydrogen Storage Materials, Springer; 1st ed. 2018 Edition, Landolt-Börnstein: Numerical Data and Functional Relationships in Science and Technology - New Series (8), 2018.

[2] H. Putz, K. Brandenburg, Pearson's Crystal Data: Crystal Structure Database for Inorganic Compounds, version 2.3, ASM International, Materials Park, Ohio, USA and Material Phases Data System, Vitznau, Switzerland, 2019.

[3] C. Colinet, A. Pasturel, A. Percheron-Guégan, J.-C. Achard, Enthalpies of formation and hydrogenation of $La(Ni_{(1-x)}Co_x)_5$ compounds, J. Less-Common Met. 134 (1987) 109–122.

[4] A. Pasturel, F. Liautaud, C. Colinet, C. Allibert, A. Percheron-Guégan, J.C. Achard, Thermodynamic study of the $LaNi_{5-x}Cu_x$ system, J. Less-Common Met. 96 (1984) 93–97.

[5] S. De Negri, P. Solokha, A. Saccone, V. Pavlyuk, Isothermal section of the La-Ni-Zn system from 16.7 to 100 at.% La at 400°C, Intermetallics. 16 (2008) 168–178.

[6] J.-M. Joubert, J. Charton, A. Percheron-Guégan, Investigation of structural and hydrogen absorption properties in the $LaNi_{5-x}Pt_x$-H_2 system, J. Solid State Chem. 173 (2003) 379–386.

[7] C. Lartigue, A. Percheron-Guégan, J.-C. Achard, F. Tasset, Thermodynamic and structural properties of $LaNi_{5-x}Mn_x$ compounds and their related hydrides, J. Less-Common Met. 75 (1980) 23–29.

[8] J. Lamloumi, A. Percheron-Guegan, J.C. Achard, G. Jehanno, D. Givord, Study of the pseudo-binary compounds $LaNi_{5-x}Fe_x$ ($x \leq 1.2$) by X-ray diffraction, Mössbauer spectroscopy and magnetic measurements, J. Phys. (Paris). 45 (1984) 1643–1652.

[9] H. Diaz, A. Percheron-Guégan, J.-C. Achard, C. Chatillon, J.-C. Mathieu, Thermodynamic and structural properties of $LaNi_{5-y}Al_y$ compounds and their related hydrides, Int. J. Hydrogen Energy. 4 (1979) 445–454.

[10] J. Prigent, J.-M. Joubert, M. Gupta, The phase diagrams of the ternary systems La-Ni-M (M=Re, Ru, Os, Rh, Ir, Pd, Ag, Au) in the La-poor region, Intermetallics. 19 (2011) 295–301.

[11] A.N. Pirogov, A.S. Yermolenko, V.N. Dvinyaninov, V.V. Chuyev, V.V. Kelarev, Neutron diffraction investigation of the distribution of cobalt and nickel atoms over the crystal lattice sites in compounds $Y(Co_{1-x}Ni_x)_5$ and $La(Co_{1-x}Ni_x)_5$, Phys. Met. Metall. 49 (1980) 120–124.

[12] J.-C. Achard, A.-J. Dianoux, C. Lartigue, A. Percheron-Guégan, F. Tasset, Structure of Al, Cu and Si substituted $LaNi_5$ and of the corresponding ß-deuterides from powder neutron

diffraction. Localized diffusion mode of hydrogen in $LaNi_5$ and Al and Mn substituted compounds from quasielastic neutron scattering, in: G.J. McCarthy, H.B. Silber, J.J. Rhyne (Eds.), Plenum, 1982: pp. 481–486.
[13] J.M. Joubert, M. Latroche, R.C. Bowman, A. Percheron-Guégan, F. Bourée-Vigneron, Structural study of the $LaNi_{4.6}Ge_{0.4}$-D_2 system using X-ray and neutron powder diffraction, Appl. Phys. A: Mater. Sci. Process. 74 (2002) S1037–S1039. https://doi.org/10.1007/s003390101189.
[14] J.-M. Joubert, M. Latroche, R. Cerný, R.C. Bowman Jr, A. Percheron-Guégan, K. Yvon, Crystallographic study of $LaNi_{5-x}Sn_x$ (0.2<=x<=0.5) compounds and their hydrides, J. Alloys Compd. 293–295 (1999) 124–129.
[15] J.-M. Joubert, R. Cerný, M. Latroche, A. Percheron-Guégan, K. Yvon, Site occupancies in the battery electrode material $LaNi_{3.55}Mn_{0.4}Al_{0.3}Co_{0.755}$ as determined by multiwavelength synchrotron powder diffraction, J. Appl. Crystallogr. 31 (1998) 327–332.
[16] Y. Nakamura, K. Oguro, I. Uehara, E. Akiba, X-ray diffraction peak broadening and lattice strain in $LaNi_5$-based alloys, J. Alloys Compd. 298 (2000) 138–145.
[17] A. Pasturel, C. Chatillon-Colinet, A. Percheron Guegan, J.C. Achard, Thermodynamic properties of $LaNi_4M$ compounds and their related hydrides, J. Less-Common Met. 84 (1982) 73–78.
[18] K.H.J. Buschow, A.S. Van Der Goot, Composition and crystal stucture of hexagonal Cu-rich rare earth-copper compounds, Acta Crystallogr. B. 27 (1971) 1085–1088.
[19] J.-M. Joubert, R. Černý, M. Latroche, E. Leroy, L. Guénée, A. Percheron-Guégan, K. Yvon, A structural study of the homogeneity domain of $LaNi_5$, J. Solid State Chem. 166 (2002) 1–6. https://doi.org/10.1006/jssc.2001.9499.
[20] R. Černý, Y. Filinchuk, S. Brühne, Local atomic order in the vicinity of Cu_2 dumbbells in $TbCu_7$-type $YCu_{6.576}$ studied by Bragg and total scattering techniques, Intermetallics. 17 (2009) 818–825.
[21] F. Cuevas, M. Latroche, M. Hirscher, A. Percheron-Guégan, Formation and structure of highly over-stoichiometric $LaNi_{5+x}$($x\sim1$) alloys obtained by manifold non-equilibrium methods, Journal of Alloys and Compounds. 323–324 (2001) 4–7. https://doi.org/10.1016/S0925-8388(01)01004-0.
[22] F. Cuevas, M. Hirscher, B. Ludescher, H. Kronmüller, Preparation of highly overstoichiometric $LaNi_{5+x}$($1\leqslant x\leqslant4$) single-phase films by ion beam sputtering, Journal of Applied Physics. 86 (1999) 6690–6696. https://doi.org/10.1063/1.371745.
[23] A.C. Switendick, Band structure calculations for metal hydrogen systems, Z. Phys. Chem. Neue Folge. 117 (1979) 89–112.
[24] D.G. Westlake, Site occupancies and stoichiometries in hydrides of intermetallic compounds : geometric considerations, J. Less-Common Met. 90 (1983) 251–273.
[25] C. Crowder, W.J. James, W. Yelon, A powder neutron diffraction study of the $LaNi_{4.5}Al_{0.5}D_{4.5}$ structure at 298 and 77 °K, J. Appl. Phys. 53 (1982) 2637–2639.
[26] J. Lamloumi, A. Percheron-Guégan, C. Lartigue, J.-C. Achard, G. Jehanno, Thermodynamic structural and magnetic properties of $LaNi_{5-x}Fe_x$ hydrides, J. Less-Common Met. 130 (1987) 111–122.
[27] Y. Nakamura, K. Sakaki, H. Kim, K. Asano, T. Watanuki, A. Machida, Reaction paths via a new transient phase in non-equilibrium hydrogen absorption of $LaNi_2Co_3$, International Journal of Hydrogen Energy. 45 (2020) 21655–21665.
[28] Y. Nakamura, T. Ishigaki, T. Kamiyama, E. Akiba, Crystal structure and hydrogen occupation of $LaNi_{4.9}Al_{0.1}D_x$ (5.0< x < 6.1) on the desorption isotherm studied by in situ neutron powder diffraction, J. Alloys Compd. 384 (2004) 195–202.
[29] A. Percheron-Guégan, C. Lartigue, J.-C. Achard, P. Germi, F. Tasset, Neutron and X-ray diffraction profile analyses and structure of $LaNi_5$, $LaNi_{5-x}Al_x$ and $LaNi_{5-x}Mn_x$ intermetallics and their hydrides (deuterides), J. Less-Common Met. 74 (1980) 1–12.
[30] J. Prigent, J.-M. Joubert, M. Gupta, Investigation of modification of hydrogenation and structural properties of $LaNi_5$ intermetallic compound induced by substitution of Ni by Pd, J. Solid State Chem. 184 (2011) 123–133.
[31] C. Lartigue, A. Percheron-Guégan, J.-C. Achard, J.-L. Soubeyroux, Hydrogen (deuterium) ordering in the ß-$LaNi_5D_x$ phases: a neutron diffraction study, J. Less-Common Met. 113 (1985) 127–148.
[32] Y. Nakamura, R. Bowman, E. Akiba, Variation of hydrogen occupation in $LaNi_{4.78}Sn_{0.22}D_x$ along P-C isotherms studied by in situ neutron powder diffraction, J. Alloys Compd. 431 (2007) 148–154. https://doi.org/10.1016/j.jallcom.2006.05.082.

[33] C. Lartigue, A. Le Bail, A. Percheron-Guégan, A new study of the structure of $LaNi_5D_{6.7}$ using a modified Rietveld method for the refinement of neutron powder diffraction data, J. Less-Common Met. 129 (1987) 65–76.
[34] P. Thompson, J. J. Reilly, L. M. Corliss, J. M. Hastings, R. Hempelmann, The crystal structure of $LaNi_5D_7$, J. Phys. F., Met. Phys. 16 (1986) 675–685.
[35] M. Latroche, J.-M. Joubert, A. Percheron-Guégan, F. Bourée-Vigneron, Neutron diffraction study of the deuterides of the over-stoichiometric compounds $LaNi_{5+x}$, J. Solid State Chem. 177 (2004) 1219–1229.
[36] M. Latroche, R.C. Bowman, Crystal structure of the deuteride $LaCu_5D_{3.2}$ studied by neutron powder diffraction, J. Alloys Compd. 446–447 (2007) 11–14.
[37] J.-M. Joubert, M. Latroche, A. Percheron-Guégan, Metallic Hydrides II: Materials for Electrochemical Storage, MRS Bull. 27 (2002) 694–698. https://doi.org/10.1557/mrs2002.224.
[38] E. Akiba, K. Nomura, S. Ono, A new hydride phase of $LaNi_5H_3$, J. Less-Common Met. 129 (1987) 159–164.
[39] S. Luo, J.D. Clewley, T.B. Flanagan, R.C. Bowman Jr., L.A. Wade, Further studies of the isotherms of $LaNi_{5-x}Sn_x$-H for x=0-0.5, J. Alloys Compd. 267 (1998) 171–181. https://doi.org/10.1016/S0925-8388(97)00536-7.
[40] V.A. Yartys, R.V. Denys, C.J. Webb, J.P. Mæhlen, E.MacA. Gray, T. Blach, O. Isnard, L.C. Barnsley, High pressure in situ diffraction studies of metal–hydrogen systems, Journal of Alloys and Compounds. 509 (2011) S817–S822. https://doi.org/10.1016/j.jallcom.2010.12.030.
[41] H. Diaz, Etude du système $LaNi_{5-x}Al_xH_y$. Application au stockage de l'énergie, Thèse de docteur-ingénieur, Université Pierre et Marie Curie, 1978.
[42] L. Vegard, Die Konstitution der Mischkristalle und die Raumfüllung der Atome, Z. Phys. Chem. Neue Folge. 5 (1921) 17–26.
[43] A. Percheron-Guégan, C. Lartigue, J.-C. Achard, Correlations between the structural properties, the stability and the hydrogen content of substituted $LaNi_5$ compounds, J. Less-Common Met. 109 (1985) 287–309.
[44] J.-C. Achard, A. Percheron-Guégan, H. Diaz, F. Briaucourt, F. Demany, Rare earth ternary hydrides. Hydrogen storage applications, 2nd Int. Congress on Hydrogen in Metals. (1977) 1E12.
[45] M.H. Mendelsohn, D.M. Gruen, A.E. Dwight, The effect of aluminum additions on the structural and hydrogen absorption properties of AB_5 alloys with particular reference to the $LaNi_{5-x}Al_x$ ternary alloy system, J. Less-Common Met. 63 (1979) 193–207.
[46] M.H. Mendelsohn, D.M. Gruen, A.E. Dwight, $LaNi_{5-x}Al_x$ is a versatile alloy system for metal hydride applications, Nature. 269 (1977) 45–47.
[47] J. Prigent, J.-M. Joubert, M. Gupta, Modification of the hydrogenation properties of $LaNi_5$ upon Ni substitution by Rh, Ir, Pt or Au, J. Alloys Compd. 511 (2012) 95–100.
[48] X. Wang, C. Wang, C. Chen, Q. Wang, Stability of AB_5-type hydrogen storage alloys, J. Alloys Compd. 420 (2006) 107–110.
[49] J.F. Lakner, F.S. Uribe, S.A. Steward, Hydrogen and deuterium sorption by selected rare earth intermetallic compounds at pressures up to 1500 atm, J. Less-Common Met. 72 (1980) 87–105. https://doi.org/10.1016/0022-5088(80)90255-6.
[50] S.N. Klyamkin, V.N. Verbetsky, Interaction of intermetallic compounds with hydrogen at pressures up to 250 MPa: the $LaCo_{5-x}Mn_x$-H_2 and $CeNi_5$−H_2 systems, J. Alloys Compd. 194 (1993) 41–45. https://doi.org/10.1016/0925-8388(93)90642-Z.
[51] E. Burzo, A. Chelkowski, H.R. Kirchmayr, Compounds between Rare earth Elements and 3d, 4d, 5d elements, in: H. P.J. Wijn (Ed.), Magnetic Properties of Metal, Landolt-Börstein, Springer Verlag, Berlin, 1990.
[52] D. Gignoux, D. Schmitt, Magnetic properties of intermetallic compounds, in: J. Gschneidner, J. and L. Eyring (Eds.), Handbook of the Physics and Chemistry of Rare Earths, Elsevier Science B.V., 1995: pp. 293–424.
[53] G. Wiesinger, G. Hilscher, Magnetism of hydrides, in: K.H.J. Buschow (Ed.), Handbook of Magnetic Materials, Elsevier North-Holland, Amsterdam, 2008: pp. 293–456.
[54] G. Wiesinger, G. Hilscher, Magnetism of hydrides, in: K.H.J. Buschow (Ed.), Handbook of Magnetic Materials, Elsevier North-Holland, Amsterdam, 1991: p. 511.
[55] G. Wiesinger, G. Hilsher, Hydrogen in Intermetallic compounds I, in: L. Schlapbach (Ed.), Topics in Applied Physics, Springer-Verlag, Berlin, 1988: p. 285.
[56] P.C.M. Gubbens, A.M. Vanderkraan, Magnetic-Properties of $ThFe_5$, Journal of Magnetism and Magnetic Materials. 9 (1978) 349–354.

[57] P.C.M. Gubbens, A.M. Vanderkraan, K.H.J. Buschow, Fe-^{57} Mossbauer-Effect in $ThFe_5$ Hydride, Journal of Applied Physics. 56 (1984) 2547–2552.
[58] G. Hoffer, K. Strnat, Magnetocrystalline Anisotropy of YCo_5 and Y_2Co_{17}, IEEE Transactions on Magnetics. 2 (1966) 487–489.
[59] J. Ormerod, Rare Earth Magnets: Yesterday, Today And Tomorrow, Orlando, FL, USA, 2019. https://fr.slideshare.net/JohnOrmerod/2019-01-17-magnetics-2019.
[60] K.J. Strnat, R.M.W. Strnat, Rare earth-cobalt permanent magnets, Journal of Magnetism and Magnetic Materials. 100 (1991) 38–56.
[61] G.H.O. Daalderop, P.J. Kelly, M.F.H. Schuurmans, Magnetocrystalline anisotropy of YCo_5 and related $RECo_5$ compounds, Physical Review B. 53 (1996) 14415–14433.
[62] L. Steinbeck, M. Richter, H. Eschrig, Magnetocrystalline anisotropy of RCo_5 intermetallics: itinerant-electron contribution, Journal of Magnetism and Magnetic Materials. 226 (2001) 1011–1013.
[63] L. Steinbeck, M. Richter, H. Eschrig, Itinerant-electron magnetocrystalline anisotropy energy of YCo_5 and related compounds, Physical Review B. 63 (2001) 184431.
[64] J. Schweizer, F. Tasset, Polarized Neutron Study of the RCo_5 Intermetallic Compounds .1. the Cobalt Magnetization in YCo_5, Journal of Physics F-Metal Physics. 10 (1980) 2799–2817.
[65] J.M. Alameda, D. Givord, R. Lemaire, Q. Lu, Co Energy and Magnetization Anisotropies in RCo_5 Intermetallics between 4.2-K and 300-K, Journal of Applied Physics. 52 (1981) 2079–2087.
[66] M. Yamaguchi, T. Katamune, T. Ohta, Magnetic studies of hydride phase transformations in $NdCo_5H_x$, $PrCo_5Hx$ and $LaCo_5H_x$, J. Less-Common Met. 88 (1982) 195–200.
[67] M. Yamaguchi, T. Katamune, T. Ohta, Magnetic-Behavior of Metal-Hydrides as a Function of Hydrogen Pressure and Composition, Journal of Applied Physics. 53 (1982) 2788–2792.
[68] F.A. Kuijpers, B.O. Loopstra, A neutron-diffraction study on the structural relationships of RCo_5 hydrides, J. Phys. Chem. Solids. 35 (1974) 301–306.
[69] M. Yamaguchi, T. Ohta, Y. Osumi, Magnetic behavior of $SmCo_5$-hydrogen system, Journal of Magnetism and Magnetic Materials. 35 (1983) 114–116. https://doi.org/10.1016/0304-8853(83)90469-9.
[70] M. Yamaguchi, T. Ohta, T. Katayama, Effect of hydrogen absorption on magnetic properties of $GdCo_5$ and YCo_5, Journal of Magnetism and Magnetic Materials. 31–34 (1983) 221–222.
[71] G. Herbst, H. Krönmuller, Magnetic Orientation Aftereffect of Hydrogen Isotopes in Rare-Earth - Cobalt Alloys, Zeitschrift Fur Physikalische Chemie-Wiesbaden. 116 (1979) 31–38.
[72] G. Herbst, H. Krönmuller, Magnetic Aftereffect of Hydrogen and Deuterium in Co_5Sm, Physics Letters A. 70 (1979) 341–343.
[73] M. Yamaguchi, S. Sasaki, T. Ohta, Nuclear Magnetic-Resonance Studies of Ferromagnetic Hydrides Based on Rare Earth-Cobalt Intermetallics - the Effect of Hydrogen on Spectra of the Hyperfine Field at Co-59 Nuclei in $GdCo_5H_x$ and YCo_5H_x, J. Less-Common Met. 73 (1980) 201–205.
[74] H. Figiel, Comments on Nuclear Magnetic-Resonance Studies of $GdCo_5H_x$ and YCo_5H_x Hydrides, J. Less-Common Met. 83 (1982) L27–L28.
[75] R.G. Barnes, W.C. Harper, S.O. Nelson, D.K. Thome, D.R. Torgeson, Investigation of Systems $LaNi_5H_x$ and $LaNi_5D_x$ by Proton and Deuteron Nuclear Magnetic-Resonance, J. Less-Common Met. 49 (1976) 483–502.
[76] T.P. Blach, E.M. Gray, Magnetic properties of the $LaNi_5$-H system, Journal of Alloys and Compounds. 253 (1997) 336–338.
[77] M. Gupta, Electronic properties of $LaNi_5$ and $LaNi_5H_7$, J. Less-Common Met. 130 (1987) 219–227.
[78] S.F. Matar, Intermetallic hydrides: A review with ab initio aspects, Progress in Solid State Chemistry. 38 (2010) 1–37.
[79] W.E. Wallace, H.E. Flotow, D. Ohlendorf, Configurational Entropy and Structure of ß-$LaNi_5$ Hydride, J. Less-Common Met. 79 (1981) 157–160.
[80] D. Ohlendorf, H.E. Flotow, Heat-Capacities and Thermodynamic Functions of $LaNi_5$, $LaNi_5H_{0.36}$ and $LaNi_5H_{6.39}$ from 5 to 300 K, J. Less-Common Met. 73 (1980) 25–32.
[81] L. Schlapbach, Magnetic properties of $LaNi_5$ and their variation with hydrogen absorption and desorption, J. Phys. F: Met. Phys. 10 (1980) 2477.
[82] L. Schlapbach, F. Stucki, A. Seiler, H.C. Siegmann, Magnetism and Hydrogen Storage in $LaNi_5$, FeTi and Mg_2Ni, Journal of Magnetism and Magnetic Materials. 15–8 (1980) 1271–1272.

[83] L. Schlapbach, A. Seiler, H.C. Siegmann, T.V. Waldkirch, P. Zurcher, C.R. Brundle, Self Restoring of the Active Surface in $LaNi_5$, International Journal of Hydrogen Energy. 4 (1979) 21–28.
[84] D. Gignoux, A. Naitsaada, R. Perrier de labathie, Magnetic-Properties of $TbNi_5$ and $HoNi_5$ Single-Crystals, Journal de Physique. 40 (1979) 188–190.
[85] G. Aubert, D. Gignoux, B. Hennion, B. Michelutti, A.N. Saada, Bulk magnetization study of a $DyNi_5$ single crystal, Solid State Communications. 37 (1981) 741–743.
[86] P. Svoboda, J. Vejpravovvá, N.T.H. Kim-Ngan, F. Kaysel, Specific heat study of selected RNi_5, Journal of Magnetism and Magnetic Materials. 272–276 (2004) 595–596.
[87] P.J. von Ranke, M.A. Mota, D.F. Grangeia, A.M.G. Carvalho, F.C.G. Gandra, A.A. Coelho, A. Caldas, N.A. de Oliveira, S. Gama, Magnetocaloric effect in the RNi_5 (R = Pr, Nd, Gd, Tb, Dy, Ho, Er) series, Physical Review B. 70 (2004) 134428.
[88] M. Escorne, A. Mauger, J. Lamloumi, A. Percheron-Guégan, Local Versus Long-Range Magnetic-Ordering in $LaNi_{5-x}Fe_x$, Solid State Communications. 89 (1994) 761–765.
[89] M. Escorne, J. Lamloumi, A. Percheron-Guégan, J.C. Achard, A. Mauger, G. Jehanno, Magnetic Clustering in $LaNi_{5-x}Fe_x$ Compounds, Journal of Applied Physics. 63 (1988) 4121–4123.
[90] M. Escorne, J. Lamloumi, A. Percheron-Guégan, J.C. Achard, A. Mauger, Spin Freezing Properties in $LaNi_{5-x}Fe_x$, Journal of Magnetism and Magnetic Materials. 65 (1987) 63–70.
[91] V. Paul-Boncour, M. Gupta, J.-M. Joubert, A. Percheron-Guégan, P. Parent, C. Laffon, Investigation of the electronic properties of substituted $LaNi_5$ compounds used as material for batteries, Journal of Materials Chemistry. 10 (2000) 225–238.
[92] E.W. Jungner, Elektriskt primär- eller sekundärelement, FI1071 (A), 1899. https://worldwide.espacenet.com/publicationDetails/biblio?FT=D&date=18991019&DB=EPODOC&locale=en_EP&CC=FI&NR=1071A&KC=A&ND=4#.
[93] E.W. Justi, H.H. Ewe, A.W. Kalberlah, N.M. Saridakis, M.H. Schaefer, Electrocatalysis in the nickel-titanium System, Energy Conversion. 10 (1970) 183–187.
[94] H.H. Ewe, E.W. Justi, K. Stephan, Elektrochemische Speicherung und Oxidation von Wasserstoff mit der intermetallischen Verbindung $LaNi_5$, Energy Conversion. 13 (1973) 109–113.
[95] J.H.N. Van Vucht, F.A. Kuijpers, H.C.A.M. Bruning, Reversible room-temperature absorption of large quantities of hydrogen by intermetallic compounds, Philips Res. Rep. 25 (1970) 133–140.
[96] F.G. Will, Hermetically sealed secondary battery with lanthanum nickel anode, US3874928 (A), 1975.
[97] J.J.G. Willems, Metal hydride electrodes stability of $LaNi_5$-related compounds, Philips J. Res. 39 (1984) 1–94.
[98] G. Bronoël, J. Sarradin, M. Bonnemay, A. Percheron-Guégan, J.-C. Achard, L. Schlapbach, A new hydrogen storage electrode, Int. J. Hydrogen Energy. 1 (1976) 251–254.
[99] A. Percheron Guégan, J.-C. Achard, J. Loriers, M. Bonnemay, G. Bronoël, J. Sarradin, L. Schlapbach, Electrode materials based on lanthanum and nickel, and electrochemical uses of such materials, US4107405 (A), 1978. https://worldwide.espacenet.com/publicationDetails/originalDocument?CC=US&NR=4107405A&KC=A&FT=D&ND=3&date=19780815&DB=EPODOC&locale=en_EP.
[100] A. Percheron-Guégan, J.-C. Achard, J. Sarradin, G. Bronoël, Electrode Material based on Lanthanum and Nickel, Electrochemical uses of such materials., US patent 4 688 537, 1978.
[101] A. Percheron-Guégan, J.-C. Achard, J. Sarradin, G. Bronoël, Hydrogen electrochemical storage by substituted $LaNi_5$ compounds, in: A.F. Andersen, A.J. Maeland (Eds.), Proceedings of an International Symposium Held in Geilo, Norway, 14–19 August 1977, Pergamon Press, Oxford, Geilo, Norway, 1978: pp. 485–490. https://doi.org/10.1016/B978-0-08-022715-3.50043-6.
[102] A. Percheron-Guégan, J.-C. Achard, J. Sarradin, G. Bronoël, Alliages à base de Lanthane et de Nickel et leurs applications électrochimiques, French patent 77 23812, 1977.
[103] A. Percheron-Guégan, J.-C. Achard, J. Sarradin, G. Bronoël, Alliages à base de Lanthane et de Nickel et leurs applications électrochimiques, French patent 75 16160, 1975.
[104] H. Züchner, T. Rauf, R. Hempelmann, Electrochemical measurements of hydrogen diffusion in the intermetallic compound $LaNi_5$, J. Less-Common Met. 172–174 (1991) 611–617. https://doi.org/10.1016/0022-5088(91)90182-4.
[105] H. Ogawa, M. Ikoma, H. Kawano, I. Matsumoto, Metal hydride electrode for high energy density sealed nickel-metal hydride battery, J. Power Sources. 12 (1988) 393–410.

[106] V. Paul-Boncour, J.-M. Joubert, M. Latroche, A. Percheron-Guegan, In situ XAS study of the hydrogenation of AB_5 compounds (A=La, Ce, and B=$Ni_{3.55}Mn_{0.4}Al_{0.3}Co_{0.75}$), J. Alloys Compd. 330–332 (2002) 246–249.
[107] F. Maurel, B. Knosp, M. Backhaus-Ricoult, Characterization of corrosion products of AB_5-type hydrogen storage alloys for nickel-metal hydride batteries, J. Electrochem. Soc. 147 (2000) 78–86.
[108] M. Latroche, A. Percheron-Guegan, Y. Chabre, Influence of cobalt content in $MmNi_{4.3-x}Mn_{0.3}Al_{0.4}Co_x$ alloy (x=0.36 and 0.69) on its electrochemical behaviour studied by in situ neutron diffraction, J. Alloys Compd. 293–295 (1999) 637–642.
[109] M. Latroche, Y. Chabre, A. Percheron-Guegan, O. Isnard, B. Knosp, Influence of stoichiometry and composition on the structural and electrochemical properties of AB_{5+y}-based alloys used as negative electrode materials in Ni-MH batteries., J. Alloys Compd. 330–332 (2002) 787–791. https://doi.org/10.1016/S0925-8388(01)01490-6.
[110] S. Vivet, M. Latroche, Y. Chabre, J.-M. Joubert, B. Knosp, A. Percheron-Guegan, Influence of composition on phase occurrence during charge process of AB_{5+x} Ni-MH negative electrode materials, Physica B: Condensed Matter. 362 (2005) 199–207.
[111] S. Vivet, J.-M. Joubert, B. Knosp, A. Percheron-Guégan, Effects of cobalt replacement by nickel, manganese, aluminium and iron on the crystallographic and electrochemical properties of AB_5-type alloys, J. Alloys Compd. 356–357 (2003) 779–789.
[112] S. Vivet, J.-M. Joubert, B. Knosp, P. Ochin, A. Percheron Guegan, The effect of over-stoichiometry on the electrochemical properties of $LaNi_5$ derived electrode materials, J. Alloy Compd. 465 (2008) 217–521. https://doi.org/10.1016/j.jallcom.2007.10.133.
[113] D.P. Broom, M. Kemali, D.K. Ross, Magnetic properties of commercial metal hydride battery materials, J. Alloys Compd. 293–295 (1999) 255–259.
[114] M. Ayari, V. Paul-Boncour, J. Lamloumi, A. Percheron-Guégan, M. Guillot, Study of the aging of $LaNi_{3.55}Mn_{0.4}Al_{0.3}(Co_{1-x}Fe_x)_{0.75}$ (0 <= x <=1) compounds in Ni-MH batteries by SEM and Magnetic measurements, J. Magn. Magn. Mater. 288 (2005) 374–383.
[115] M. Ayari, V. Paul-Boncour, J. Lamloumi, A. Percheron-Guégan, Decomposition of the $LaNi_{3.55}Mn_{0.4}Al_{0.3}Fe_{0.75}$ compound upon electrochemical cycling studied by magnetic properties, J. Alloys Compd. 356–357 (2003) 133–136.
[116] M. Ayari, V. Paul-Boncour, J. Lamloumi, A. Percheron-Guégan, Magnetic properties of $LaNi_{3.55}Mn_{0.4}Al_{0.3}Co_{0.75-x}Fe_x$ (x=0,0.35) before and after electrochemical cycles, J. Magn. Magn. Mat. 242–245 (2002) 850–853.
[117] F. Cuevas, J.-M. Joubert, M. Latroche, A. Percheron-Guégan, Intermetallic compounds as negative electrodes of Ni/MH batteries, Appl. Phys. A. 72 (2001) 225–238.
[118] J.-C. Crivello, J. Zhang, M. Latroche, Structural Stability of ABy Phases in the (La,Mg)–Ni System Obtained by Density Functional Theory Calculations, J. Phys. Chem. C. 115 (2011) 25470–25478. https://doi.org/10.1021/jp204835z.
[119] T. Kohno, H. Yoshida, F. Kawashima, T. Inaba, I. Sakai, M. Yamamoto, M. Kanda, Hydrogen storage properties of new ternary system alloys: La_2MgNi_9, $La_5Mg_2Ni_{23}$, La_3MgNi_{14}, J. Alloys Compd. 311 (2000) L5–L7.
[120] V. Charbonnier, N. Madern, J. Monnier, J. Zhang, V. Paul-Boncour, Michel. Latroche, Relationship between H2 sorption, electrochemical cycling and aqueous corrosion properties in A_5Ni_{19} hydride-forming alloys (*A* = Gd, Sm)., J. Power Sources. 397 (2018) 280–287. https://doi.org/10.1016/j.jpowsour.2018.07.033.
[121] L. Lemort, M. Latroche, B. Knosp, P. Bernard, Elaboration and characterization of new pseudo-binary hydride-forming phases $Pr_{1.5}Mg_{0.5}Ni_7$ and $Pr_{3.75}Mg_{1.25}Ni_{19}$: A comparison to the binary Pr_2Ni_7 and Pr_5Ni_{19} ones, J. Phys. Chem. C. 115 (2011) 19437–19444.
[122] P.H.L. Notten, M. Latroche, Secondary Batteries: Nickel Batteries Metal Hydride Alloys, in: J. Garche (Ed.), Encyclopedia of Electrochemical Power Sources, Elsevier, Amsterdam, 2009: pp. 502–521.
[123] V. Yartys, D. Noreus, M. Latroche, Metal hydrides as negative electrode materials for Ni–MH batteries, Appl. Phys. A. 122 (2016) 43. https://doi.org/10.1007/s00339-015-9538-9.
[124] R.V. Denys, V.A. Yartys, E.M. Gray, C.J. Webb, LaNi5-Assisted Hydrogenation of MgNi2 in the Hybrid Structures of La1.09Mg1.91Ni9D9.5 and La0.91Mg2.09Ni9D9.4, Energies. 8 (2015) 3198–3211. https://doi.org/10.3390/en8043198.
[125] F.E. Lynch, Metal hydride practical applications, Journal of the Less Common Metals. 172–174 (1991) 943–958. https://doi.org/10.1016/S0022-5088(06)80001-9.

[126] G. Sandrock, R.C. Bowman, Gas-based hydride applications: recent progress and future needs, Journal of Alloys and Compounds. 356–357 (2003) 794–799. https://doi.org/10.1016/S0925-8388(03)00090-2.
[127] G. Sandrock, A panoramic overview of hydrogen storage alloys from a gas reaction point of view, Journal of Alloys and Compounds. 293–295 (1999) 877–888. https://doi.org/10.1016/S0925-8388(99)00384-9.
[128] K. Kubo, Y. Kawaharazaki, H. Itoh, Development of large MH tank system for renewable energy storage, International Journal of Hydrogen Energy. 42 (2017) 22475–22479. https://doi.org/10.1016/j.ijhydene.2017.06.048.
[129] P. Bhandari, M. Prina, R.C. Bowman, C. Paine, D. Pearson, A. Nash, Sorption coolers using a continuous cycle to produce 20 K for the Planck flight mission, Cryogenics. 44 (2004) 395–401. https://doi.org/10.1016/j.cryogenics.2004.02.022.
[130] H-Bank Hydrogen Storage Solutions, (2020). http://www.hbank.com.tw/about.html (accessed October 9, 2020).
[131] The Japan Steel Works, LTD., (2020). https://www.jsw.co.jp/en/product/new_business/hydrogen.html (accessed October 9, 2020).
[132] Pragma-Industries stockage hydrogene, Pragma Industries. (2020). https://www.pragma-industries.com/fr/stockage-hydrogene/ (accessed October 9, 2020).
[133] MaHyTec-Solid hydrogen storage, MAHYTEC. (2020). https://www.mahytec.com/en/products/solid-hydrogen-storage/ (accessed October 9, 2020).
[134] Hydrogen Components, INC., (2020). http://www.hydrogencomponents.com/index.htm (accessed October 9, 2020).
[135] Ergenics, (2020). http://ergenics.com/ha.html (accessed October 9, 2020).
[136] E.L. Huston, G.D. Sandrock, Engineering properties of metal hydrides, Journal of the Less Common Metals. 74 (1980) 435–443. https://doi.org/10.1016/0022-5088(80)90182-4.
[137] S.H. Kim, C.M. Miesse, H.B. Lee, I.W. Chang, Y.S. Hwang, J.H. Jang, S.W. Cha, Ultra compact direct hydrogen fuel cell prototype using a metal hydride hydrogen storage tank for a mobile phone, Applied Energy. 134 (2014) 382–391. https://doi.org/10.1016/j.apenergy.2014.08.019.
[138] G. Han, Y. Kwon, J.B. Kim, S. Lee, J. Bae, E. Cho, B.J. Lee, S. Cho, J. Park, Development of a high-energy-density portable/mobile hydrogen energy storage system incorporating an electrolyzer, a metal hydride and a fuel cell, Applied Energy. 259 (2020) 114175. https://doi.org/10.1016/j.apenergy.2019.114175.
[139] Mahytec's hydrogen tanks power the first use of hydrogen for the general public at a country scale, MAHYTEC. (2016). https://www.mahytec.com/en/mahytec-hydrogen-tanks-power-the-first-use-of-hydrogen-for-the-general-public-at-a-country-scale/ (accessed October 9, 2020).
[140] Iwatani Corporation, (2009). http://www.iwatani.co.jp/eng/newsrelease/detail_32.html (accessed October 9, 2020).
[141] M.V. Lototskyy, I. Tolj, M.W. Davids, Y.V. Klochko, A. Parsons, D. Swanepoel, R. Ehlers, G. Louw, B. van der Westhuizen, F. Smith, B.G. Pollet, C. Sita, V. Linkov, Metal hydride hydrogen storage and supply systems for electric forklift with low-temperature proton exchange membrane fuel cell power module, International Journal of Hydrogen Energy. 41 (2016) 13831–13842. https://doi.org/10.1016/j.ijhydene.2016.01.148.
[142] S.S. Bhogilla, H. Ito, T. Segawa, A. Kato, A. Nakano, Experimental study on laboratory scale totalized hydrogen energy utilization system using wind power data, International Journal of Hydrogen Energy. 42 (2017) 13827–13838. https://doi.org/10.1016/j.ijhydene.2016.12.125.
[143] M. Bielmann, U.F.Vogt, M. Zimmermann, A. Züttel, Seasonal energy storage system based on hydrogen for self sufficient living, Journal of Power Sources. 196 (2011) 4054–4060. https://doi.org/10.1016/j.jpowsour.2010.11.096.
[144] P. Rizzi, E. Pinatel, C. Luetto, P. Florian, A. Graizzaro, S. Gagliano, M. Baricco, Integration of a PEM fuel cell with a metal hydride tank for stationary applications, Journal of Alloys and Compounds. 645 (2015) S338–S342. https://doi.org/10.1016/j.jallcom.2014.12.145.
[145] Hydrogen-based Autonomous Energy Supply System H2One™, (2020). https://www.toshiba-energy.com/en/hydrogen/product/h2one.htm (accessed October 9, 2020).
[146] H.H. van Mal, A $LaNi_5$-hydride thermal absorption compressor for a hydrogen refrigerator, Chemie Ingenieur Technik. 45 (1973) 80–83. https://doi.org/10.1002/cite.330450207.
[147] R.C. Bowman, Development of metal hydride beds for sorption cryocoolers in space applications, Journal of Alloys and Compounds. 356–357 (2003) 789–793. https://doi.org/10.1016/S0925-8388(03)00089-6.

[148] R.C. Bowman Jr, Metal Hydride Compressors with Gas-Gap Heat Switches: Concept, Development, Testing, and Space Flight Operation for the Planck Sorption Cryocoolers, Inorganics. 7 (2019) 139. https://doi.org/10.3390/inorganics7120139.
[149] R.C. Bowman, B. Fultz, Metallic Hydrides I: Hydrogen storage and other gas-phase applications, MRS Bulletin. 27 (2002) 688–693. https://doi.org/10.1557/mrs2002.223.
[150] J. Bellosta von Colbe, J.-R. Ares, J. Barale, M. Baricco, C. Buckley, G. Capurso, N. Gallandat, D.M. Grant, M.N. Guzik, I. Jacob, E.H. Jensen, T. Jensen, J. Jepsen, T. Klassen, M.V. Lototskyy, K. Manickam, A. Montone, J. Puszkiel, S. Sartori, D.A. Sheppard, A. Stuart, G. Walker, C.J. Webb, H. Yang, V. Yartys, A. Züttel, M. Dornheim, Application of hydrides in hydrogen storage and compression: Achievements, outlook and perspectives, International Journal of Hydrogen Energy. 44 (2019) 7780–7808. https://doi.org/10.1016/j.ijhydene.2019.01.104.
[151] M.V. Lototskyy, V.A. Yartys, B.G. Pollet, R.C. Bowman, Metal hydride hydrogen compressors: A review, International Journal of Hydrogen Energy. 39 (2014) 5818–5851. https://doi.org/10.1016/j.ijhydene.2014.01.158.
[152] V.A. Yartys, M. Lototskyy, V. Linkov, D. Grant, A. Stuart, J. Eriksen, R. Denys, R.C. Bowman, Metal hydride hydrogen compression: recent advances and future prospects, Appl. Phys. A. 122 (2016) 415. https://doi.org/10.1007/s00339-016-9863-7.
[153] N. Endo, K. Matsumura, Y. Kawakami, M. Ishida, T. Maeda, Operation of metal hydride hydrogen storage systems for hydrogen compression using solar thermal energy, Journal of International Council on Electrical Engineering. 6 (2016) 65–71. https://doi.org/10.1080/22348972.2016.1173779.
[154] Ø. Ulleberg, J. Meyer, J. Eriksen, A. Norheim, J.C. Gjerløw, Hynor Lillestrøm: a renewable hydrogen station & technology test center, (2014). https://docplayer.net/22097567-Hynor-lillestrom-a-renewable-hydrogen-station-technology-test-center.html (accessed October 9, 2020).
[155] K. Kurosaki, T. Maruyama, K. Takahashi, H. Muta, M. Uno, S. Yamanaka, Design and development of MH actuator system, Sensors and Actuators A: Physical. 113 (2004) 118–123. https://doi.org/10.1016/j.sna.2004.03.009.
[156] S. Ino, M. Sato, A novel soft actuator using metal hydride materials and its applications in quality-of-life technology, New Developments in Biomedical Engineering. (2010). https://doi.org/10.5772/7602.
[157] A. Vanderhoff, K.J. Kim, Experimental study of a metal hydride driven braided artificial pneumatic muscle, Smart Mater. Struct. 18 (2009) 125014. https://doi.org/10.1088/0964-1726/18/12/125014.
[158] D.J. Hanley, E.L. Huston, P.M. Golben, Hydride operated reversible temperature responsive actuator and device, US5485884A, 1996. https://patents.google.com/patent/US5485884/en (accessed September 22, 2020).
[159] P. Muthukumar, A. Kumar, N.N. Raju, K. Malleswararao, M.M. Rahman, A critical review on design aspects and developmental status of metal hydride based thermal machines, International Journal of Hydrogen Energy. 43 (2018) 17753–17779. https://doi.org/10.1016/j.ijhydene.2018.07.157.
[160] M.M.H. Bhuiya, A. Kumar, K.J. Kim, Metal hydrides in engineering systems, processes, and devices: A review of non-storage applications, International Journal of Hydrogen Energy. 40 (2015) 2231–2247. https://doi.org/10.1016/j.ijhydene.2014.12.009.
[161] P. Dantzer, Metal-Hydride technology: A critical review, in: H. Wipf (Ed.), Hydrogen in Metals III: Properties and Applications, Springer, Berlin, Heidelberg, 1997: pp. 279–340. https://doi.org/10.1007/BFb0103405.
[162] M.R. Gopal, S.S. Murthy, Experiments on a metal hydride cooling system working with ZrMnFe/MmNi4.5Al0.5 pair, International Journal of Refrigeration. 22 (1999) 137–149. https://doi.org/10.1016/S0140-7007(98)00033-4.
[163] B. Satya Sekhar, P. Muthukumar, Performance tests on a double-stage metal hydride based heat transformer, International Journal of Hydrogen Energy. 38 (2013) 15428–15437. https://doi.org/10.1016/j.ijhydene.2013.09.103.
[164] M.V. Lototsky, M. Williams, V.A. Yartys, Ye.V. Klochko, V.M. Linkov, Surface-modified advanced hydrogen storage alloys for hydrogen separation and purification, Journal of Alloys and Compounds. 509 (2011) S555–S561. https://doi.org/10.1016/j.jallcom.2010.09.206.
[165] S. Miura, A. Fujisawa, M. Ishida, A hydrogen purification and storage system using metal hydride, International Journal of Hydrogen Energy. 37 (2012) 2794–2799. https://doi.org/10.1016/j.ijhydene.2011.03.150.

[166] K.D. Modibane, M. Williams, M. Lototskyy, M.W. Davids, Ye. Klochko, B.G. Pollet, Poisoning-tolerant metal hydride materials and their application for hydrogen separation from CO_2/CO containing gas mixtures, International Journal of Hydrogen Energy. 38 (2013) 9800–9810. https://doi.org/10.1016/j.ijhydene.2013.05.102.
[167] E.M. Borzone, A. Baruj, G.O. Meyer, Design and operation of a hydrogen purification prototype based on metallic hydrides, Journal of Alloys and Compounds. 695 (2017) 2190–2198. https://doi.org/10.1016/j.jallcom.2016.11.067.
[168] F.S. Yang, X.Y. Chen, Z. Wu, S.M. Wang, G.X. Wang, Z.X. Zhang, Y.Q. Wang, Experimental studies on the poisoning properties of a low-plateau hydrogen storage alloy $LaNi_{4.3}Al_{0.7}$ against CO impurities, International Journal of Hydrogen Energy. 42 (2017) 16225–16234. https://doi.org/10.1016/j.ijhydene.2017.05.131.
[169] M. Au, The recovery, purification, storage and transport of hydrogen separated from industrial purge gas by means of mobile hydride containers, International Journal of Hydrogen Energy. 21 (1996) 33–37. https://doi.org/10.1016/0360-3199(95)00044-E.
[170] J.J. Sheridan, F.G. Eisenberg, E.J. Greskovich, G.D. Sandrock, E.L. Huston, Hydrogen separation from mixed gas streams using reversible metal hydrides, Journal of the Less Common Metals. 89 (1983) 447–455. https://doi.org/10.1016/0022-5088(83)90355-7.
[171] G. Sicking, Isotope effects in metal-hydrogen systems, Journal of the Less Common Metals. 101 (1984) 169–190. https://doi.org/10.1016/0022-5088(84)90093-6.
[172] I. Lambert, A. Percheron-Guegan, J. Montel, Mesure du facteur de séparation du deutérium entre l'hydrogène et l'hydrure de l'alliage $LaNi_5$, J. Chim. Phys. 74 (1977) 380–381. https://doi.org/10.1051/jcp/1977740380.
[173] B. Andreyev, V. Shitikov, E. Magomedbekov, A. Shafiev, Isotopic effects in hydrogen-intermetallic compound systems, Journal of the Less Common Metals. 90 (1983) 161–168. https://doi.org/10.1016/0022-5088(83)90066-8.
[174] A. Yawny, G. Friedlmeier, J. Bolcich, Hydrides for hydrogen-deuterium separation, International Journal of Hydrogen Energy. 14 (1989) 587–597. https://doi.org/10.1016/0360-3199(89)90118-3.
[175] H. Sakaguchi, Y. Yagi, J. Shiokawa, G. Adachi, Hydrogen isotope separation using rare earth alloy films deposited on polymer membranes, Journal of the Less Common Metals. 149 (1989) 185–191. https://doi.org/10.1016/0022-5088(89)90484-0.
[176] Y. Ito, R. Takahashi, S. Mizusaki, I. Yamamoto, M. Yamaguchi, Magnetic field effects on the hydrogen isotope separation with metal hydrides, Science and Technology of Advanced Materials. 7 (2006) 369–372. https://doi.org/10.1016/j.stam.2006.01.008.